Backpack Energy Harvester with Human Walking Model

Yue Yuan

Thesis submitted to the faculty of the Virginia Polytechnic Institute and State University in partial fulfillment of the requirements for the degree of

Master of Science
in
Mechanical Engineering

Lei Zuo, Chair
Rolf Mueller
Robin M. Queen

02/17/2017
Blacksburg, VA

Keywords: Energy harvesting. Mechanical motion rectifier (MMR). Elastically – suspended backpack. Dynamics. Human walking model.

Backpack Energy Harvester with Human Walking Model

Yue Yuan

ABSTRACT

The objective of this thesis is to design, analyze, and fabricate an innovative backpack energy harvester for human walking. To model human walking with backpack energy harvester, a simple dual-mass model has been developed and studied first. Dual-mass model for three types of distinct harvesters were investigated, pure damping, traditional rack pinion energy harvester and our MMR based energy harvester. A comparison in the output power and human comfort between the three types of harvesters is discussed. However, the dual-mass model couldn't effectively represent human walking in real situation with sinusoidal input, like M shaped Ground Reaction Force (GRF), vertical Center of Mass (COM) motion, etc. Thus, a bipedal walking model has been proposed to simulate human walking with backpack harvester.

Experiments were conducted to compare power output and efficiency of MMR based backpack energy harvester with traditional rack pinion backpack energy harvester, and verify conclusions from the bipedal walking model that the proposed backpack energy harvester using mechanical motion rectifier (MMR) mechanism has larger power output than traditional backpack energy harvester at different walking speed. In human treadmill test, subjects were asked to wear the backpack frame which embedded with harvesters walking on a treadmill. Two walking speed, 3mph and 3.5mph, and four resistor values has been tested. The test results showed that the MMR based backpack energy harvester generated more power regardless of resistor values and walking speed. Up to 4.84W average power and instant power of 12.8W could be obtained while the subject walking on the treadmill at 3.5mph speed with MMR based backpack energy harvester.

Backpack Energy Harvester with Human Walking Model

Yue Yuan

General Audience Abstract

The objective of this thesis is to design, analyze, and fabricate an innovative backpack energy harvester for human walking. To model human walking with backpack energy harvester, a simple dual-mass model has been developed and studied first. Dual-mass model for three types of distinct harvesters were investigated, pure damping, traditional rack pinion energy harvester and our Mechanical Motion Rectifier based energy harvester. A comparison in the output power and human comfort between the three types of harvesters is discussed. In addition, a bipedal walking model has been proposed to better simulate human walking with backpack harvester than simple dual mass model.

Experiments were conducted to compare power output and efficiency of MMR based backpack energy harvester with traditional rack pinion backpack energy harvester, and verify conclusions from the bipedal walking model that the proposed backpack energy harvester using mechanical motion rectifier mechanism has larger power output than traditional backpack energy harvester at different walking speed.. Up to 4.84W average power and instant power of 12.8W could be obtained while the subject walking on the treadmill at 3.5mph speed with MMR based backpack energy harvester.

This research could make significant benefit for human live, from student walking while charging their electronics to soldiers during long time mission. This suspended load backpack could reduce load while generating electricity.

Acknowledgments

First and foremost, I would like to express my sincere appreciation to my graduate advisor, Dr. Lei Zuo, for his academic support, guidance and mentorship throughout my entire graduate life. With his ideas and suggestions, I was able to find a path to what I have achieved now. I would also like to offer my sincerest gratitude to Dr. Rolf Mueller and Dr. Robin Queen for serving on my thesis committee. I won't even be able to stand here in Virginia Tech without Dr. Mueller's recommendation and great guidance in my undergraduate study.

Thanks to Dr. Weiche Tai who have mentored me since 2016 Fall, and Mingyi Liu who helped me with experiments and will continue this project after I graduate, for their encouragement and the time we spent together to overcome difficulties in this project.

In addition, the research could not continue without great support from U.S. Army Communications – Electronics Research, Development and Engineering Center (CERDEC).

I thank my family, who continuously supported me for almost all the choices that I made for my life, my fellow labmates, Yalu Pei, Yu Pan, Yilun Liu, Changwei Liang, Sijing Guo, Xiaofan Li, Yongjia Wu, and Feng Qian, for their assistance and discussions, and all my friends, especially Dong Wang, who have made my life here much more wonderful than I expected. I wish all the best for all of you.

Contents

Abstract……..…….....ii

General audience abstract…….....iii

Acknowledgments……..……...iv

Contents……..v

List of figures……viii

List of tables…….……..…….xiii

1. Introduction……1

1.1 Motivation……1

1.2 Objectives of the Thesis……..1

1.3 Literature Review……...……2

...1.3.1 Energy harvesting from human body….....2

1.3.2 Human walking……4

1.3.3 State of art energy harvesters from human motion……5

1.4 Contributions of the Thesis……9

1.5 Thesis Organization……10

2. MMR based backpack energy harvester……...……11

2.1 Chapter Introduction……..11

2.2 The concept of Mechanical Motion Rectifier Mechanism……...……12

2.3 Design and manufacture of MMR based backpack energy harvester system…….....13

2.3.1 MMR based backpack energy harvester……..…….13

2.3.2 Suspended backpack frame……..……..14

2.3.3 Convert MMR based to traditional backpack energy harvester……...16

2.4 Modeling of MMR based backpack energy harvester…..……...……17

2.4.1 Target people group…….……..….17

2.4.2 Modeling of MMR based backpack energy harvester…….……18

2.4.3 One dof model, parameters and results of MMR based backpack harvester..…….21

2.5 Chapter Summary……23
3. Compared with traditional energy harvesters using a dual mass model 25
3.1 Chapter Introduction……25
3.2 Human walking dual mass model without energy harvester……...26
3.3 Energy harvester model with pure damping force……..……27
3.4 Traditional energy harvesters model……..……..……30
3.5 MMR based energy harvester model…….33
3.6 Human comfort comparison simulation..……35
3.6.1 Peak force……..35
3.4.2 Human energy efficiency……39
3.7 Discussion on dual mass model…….....……40
3.8 Chapter Summary……41
4. A bipedal walking with suspended load model .....……42
4.1 Chapter Introduction……42
4.2 Bipedal dynamics human walking model……..……43
4.3 Stability……46
4.4 Comparison in MMR based and traditional backpack energy harvester…..……49
4.5 Improved bipedal walking model…..……..……56
4.6 Chapter Summary……57
5. Human experiment…..……59
5.1 Chapter Introduction……59
5.2 Human test……59
5.2.1 Human test setup and procedure……..……59
5.2.2 Human test results and discussion……..……60
5.2.3 Human vertical COM results..……63
5.3 Chapter Summary……66
6. Conclusion and Future Work……66
6.1 Conclusions of the Thesis……66

6.2 Recommendations for Future Work…..……68

References……69

List of figures

Figure 1-1 Available power sources from human body and their estimated power value in watts [6]. (Not all the available sources included).....3

Figure 1-2 Terminology to describe the events of the gait cycle [15]…….……..……...5

Figure 1-3 Two types of shoe energy harvesters from MIT Media Lab [16]: (a) integration of a 31-mode piezoelectric dimorph under the heel and a PBDF stave under the ball of the foot; (b) A twin motor-generators and step-up gears embedded in a sneaker's sole…….....…….....6

Figure 1.4. Sliding mechanism of motion magnification for foot strike with force analysis [17]: (a) fully released; (b) fully pressed…….....……6

Figure 1-5 Biomechanical energy harvester from knee motion [4]: (a) two harvesters worn on each leg; (b) the chassis contains a gear train with a one-way clutch that allows engagement at knee extension and disengagement at knee flexion. …….……..….7

Figure 1-6. Prototype of the piezoelectric knee-joint energy harvester, Mag-WKEH [19]…...……8

Figure 1-7. The suspended load backpack energy harvester [5]……...……8

Figure 2-1. Concept of Mechanical Motion Rectifier: …….…...…...12

Figure 2-2. Electrical analogy for 'motion rectifier'[25]: (a) The mechanical motion rectifier with two roller clutches can be analogy to a full-wave voltage rectifier using a center-tapped transformer and two diodes; (b) motion rectifier result compared with electrical rectifier.....13

Figure 2-3. MMR based backpack energy harvester: (a) detailed design of MMR based backpack energy harvester; (b) assembled MMR based backpack energy harvester. …...……14

Figure 2-4. Design of suspended load backpack frame implemented with MMR based backpack energy harvester; (a) front view; (b) side view. ……..…...……...15

Figure 2-5. Assembled suspended load backpack frame with MMR based backpack energy harvester…….16

Figure 2-6. Traditional backpack energy harvester converted from MMR based backpack energy harvester.…….……...17

Figure 2-7 Loads carried on the march by various infantry units throughout history [29].....18

Figure 2-8 Current backpack energy harvesting application for soldiers: (a) Energy Harvesting Assault Pack (EHAP) [30]; (b) Lightning Packs [31]. ……..…….18

Figure 2-9 Modeling for regenerative shock absorber using electrical circuit [25]: (a) original, (b) simplified……...……19

Figure 2-10 One dof model of MMR based backpack energy harvester. (a) engagement system; (b) disengagement system.……...22

Figure 2-11 One dof Rotation speed result of MMR model……..…….23

Figure 3-1 Dual mass model without harvester: (a) two mass system with base excitation model for human body with elastically attached backpack; (b) when the backpack rigid attached to human body, Center of Mass (COM) vertical displacement with set parameters during steady - state is 0.0503m when A=0.0162.. ……..…….27

Figure 3-2 Dual mass vibration energy harvester model with equivalent damping force f_e. …….28

Figure 3-3 (a) average power at different tuning ratio and equivalent damping ratio ζ_e, where the mechanical damping $\zeta_m = 1\%$; (b) contours of average power at different tuning ratio and equivalent damping ratio…….....……29

Figure 3-4 (a) average power at different tuning ratio and equivalent damping ratio ζ_e, where the mechanical damping $\zeta_m = 10\%$; (b) contours of average power at different tuning ratio and equivalent damping ratio…….....……30

Figure 3-5 Dual mass vibration energy harvester model with equivalent damping force f_e and rotational inertia m_e……...…...30

Figure 3-6 Traditional energy harvester result with dual mass model (a) average power at different tuning ratio and equivalent damping ratio ζ_e, where the mechanical damping ζ_m =1%. (b) Contours of average power at different tuning ratio and equivalent damping ratio……32

Figure 3-7 Traditional energy harvester result with dual mass model (a) average power at different tuning ratio and equivalent damping ratio ζ_e, where the mechanical damping ζ_m =10%. (b) Contours of average power at different tuning ratio and equivalent damping ratio.……32

Figure 3-8 Two dof model of MMR based backpack energy harvester. (a) engaged system; (b)disengaged system…….....33

Figure 3-9 MMR based backpack energy harvester with dual mass model (a) Rotation speed of pinion and shaft when$k_2 = 2000\ N/m$ under steady state. Engaged period and disengaged period. (b) Average power at different tuning ratio and electrical damping ratio $\zeta_e = 0.02, 0.03, 0.04, 0.25\ and\ 0.5$, where the mechanical damping $\zeta_m = 1\%$……..…….33

Figure 3-10 Average power at different tuning ratio and electrical damping ratio $\zeta_e = 0.03, 0.05, 0.08, 0.1\ and\ 0.25$, where the mechanical damping $\zeta_m = 10\%$ in MMR based backpack energy harvester with dual mass model…… ….34

Figure 3-11 Peak force at different tuning ratio and electrical damping ratio ζ_e of pure damping system when $\zeta_m = 1\%$ (a) 3d contour plot; (b) 2d plot when ζ_e =0.01, 0.04, 0.1 and 0.3...36

Figure 3-12 Peak force at different tuning ratio and electrical damping ratio ζ_e of pure damping system when $\zeta_m = 10\%$ (a) 3d contour plot; (b) 2d plot when ζ_e =0.01, 0.04, 0.1 and 0.3……...36

Figure 3-13 Peak force at different tuning ratio and electrical damping ratio ζ_e of non MMR system when $\zeta_m = 1\%$ (a) 3d contour plot; (b) 2d plot when ζ_e =0.01, 0.04, 0.1 and 0.3...37

Figure 3-14 Peak force at different tuning ratio and electrical damping ratio ζ_e of non MMR system when $\zeta_m = 10\%$ (a) 3d contour plot; (b) 2d plot when ζ_e =0.01, 0.04, 0.1 and 0.3.....37

Figure 3-15 Peak force at different tuning ratio and electrical damping ratio ζ_e of MMR based harvester system when $\zeta_m = 1\%$ ……...38

Figure 3-16 Peak force at different tuning ratio and electrical damping ratio ζ_e of MMR based harvester system when $\zeta_m = 10\%$ ……38

Figure 3-17 Human harvester efficiency comparison of three systems, pure viscous system, non MMR system and MMR system at different tuning ratio when $\zeta_e = 0.2$……..40

Figure 3-12 Experiment data of load effect [13]: (a) for vertical COM motion (cm); (b) for vertical GRF (N) ……...……41

Figure 4-1 The spring-mass walking with suspended backpack model.……...……43

Figure 4-2 One dof model with sinusoidal input (a) COM result; (b) vertical GRF results. …….45

Figure 4-3 Results of bipedal walking with 15kg suspended load model under condition of α_0 =61° with initial walking speed is 1m/s and backpack system energy is 160J. (a) vertical COM result; (b) vertical GRF result. Gray area is double support phase while white area represents single support phase. (c) frequency content of vertical COM motion showed in (a)……...45

Figure 4-4 Fixed points solutions at different initial backpack energy E_2 level when initial walking speed $(v_1)_{in}$ =1m/s.(a) angle of attack α_0 with respect to initial height of spring leg $(y_1)_{in}$,(b) angle of attack α_0 with respect to initial height of backpack position $(y_2)_{in}$ (3) angle of attack α_0 with respect to initial horizontal position of human body $(x_1)_{in}$ (d) angle of attack α_0 with respect to step distance d ……..……..……..47

Figure 4-5 GRF and vertical COM motion at point shown in Figure 4-4. Point A and Point B are 61° and 67° at $(E_2)_{in}$=160J with $(v_1)_{in} = 1m/s$. (a) vertical COM motion result of point A; (b) vertical GRF result of point A; (c) vertical COM motion result of point B; (d) vertical GRF result of point B.……...…….……48

Figure 4-6 Frequency content of COM motion in different condition. (a) vertical COM motion result in frequency domain at different angle of attack when $(E_2)_{in} = 160J$ and $(v_1)_{in} = 1m/s$; (b) vertical COM motion result in frequency domain at different initial walking velocity $(E_2)_{in} = 170J$ and $\alpha_0 = 67°$; (c) vertical COM motion result in frequency domain at backpack energy level $(v_1)_{in} = 1m/s$ and $\alpha_0 = 60°$..……...…….49

Figure 4-7 One dof model (a) traditional backpack energy harvester model. (b) MMR based backpack energy harvester engagement (c) MMR based energy harvester disengagement model..……...…….……...….50

Figure 4-8 (a) output voltage of MMR based backpack energy harvester at point A with 5Ω external resistor; (b) output voltage of traditional backpack energy harvester at point A with 5Ω external resistor; (c) output voltage of MMR based backpack energy harvester at point B with 5Ω external resistor; (d) output voltage of traditional backpack energy harvester at point B with 5Ω external resistor; Point A and Point B have been shown in Figure 4-4……...……...…….……52

Figure 4-9 (a) output voltage of MMR based backpack energy harvester at point A with 5Ω external resistor; (b) output voltage of traditional backpack energy harvester at point A with 5Ω external resistor; (c) output voltage of MMR based backpack energy harvester at point B with 5Ω external resistor; (d) output voltage of traditional backpack energy harvester at point B with 5Ω external resistor; Point A and Point B have been shown in Figure 4-4 when system mechanical damping ratio ζ_m is 10% and external resistor is 5Ω ……..53

Figure 4-10 Average electrical power simulation results of two types of harvester, traditional backpack energy harvester and MMR based backpack energy harvester when $(E_2)_{in}$ =160J and mechanical damping ratio is 5%: (a) angle of attack with respect to initial height of spring leg at different initial speed; (b) angle of attack with respect to initial backpack position at different initial speed; (c) angle of attack with respect to initial human body horizontal position at different initial speed; (d) angle of attack with respect to step length at different initial speed…..…..……53

Figure 4-11 Single-sided amplitude spectrum in frequency domain comparison in maximum power difference point and minimum power difference point at all conditions consider at $(\mathrm{v}_1)_0 = 1\mathrm{m/s}$ …….55

Figure 4-12 Average power output with respect to different external resistor values in two types of harvester, MMR based backpack energy harvester and Non MMR (traditional) backpack energy harvester when system mechanical damping ratio is 10% and human walking gait input is Point B shown in Figure 4-4.…… …….55

Figure 4-13 The spring-mass walking with suspended backpack energy harvester model (improved bipedal model)..…… …….56

Figure 4-14 Average power output with respect to different external resistor values while wearing traditional backpack energy harvester in two walking speed, 2.5mph and 3mph, when initial leg length is 1m, 10% mechanical damping ratio of the harvester system, $\alpha_0 = 76°$, m_1 =80kg, m_2 =15kg, k_1 =38000 N/m, k_2 =2000 N/m and the harvester parameters are the same as previously mentioned..…… …….57

Figure 5-1 Backpack frame worn on a male. The harvester was installed in the cutout of the moving board and the racks are fixed to the fixed board……60

Figure 5-2 Traditional energy harvesting backpack tests: measured average power vs. different resistor values. The average power is calculated over an interval of 10 s ……62

Figure 5-3 Voltage output, measured relative displacement and power by subject A walking at 3mph with 5.24Ω external resistor: (a) MMR energy harvester; (b) traditional energy harvester. ……62

Figure 5-4 Measured relative displacement, voltage output and power by subject A walking at 3.5mph with 5.24Ω external resistor: (a) MMR energy harvester; (b) traditional energy harvester. ……63

Figure 5-5 Tracked average peak to peak distance of vertical COM motion of subjects from recorded videos during experiments: (a) subject A waling with 3mph with 5.24 Ω external resistor vertical peak to peak COM motion with time wearing MMR based energy harvester; (b) subject A waling with 3.5mph with 5.24 Ω external resistor vertical peak to peak COM motion with time wearing MMR based energy harvester; (c) subject A waling with 3mph with 5.24 Ω external resistor vertical peak to peak COM motion with time wearing traditional energy harvester; (d) subject A waling with 3.5mph with 5.24 Ω external resistor vertical peak to peak COM motion with time wearing traditional energy harvester.....65

List of tables

Table 2-1 Parameters for 1 dof model ……22

Table 4-1 Parameters values for model of walking with suspended load backpack ……44

Table 5-1 Concluded results of dual mass model, bipedal model and experimental results.....…66

1. Introduction

1.1 Motivation

With increasing need of portable electronics, such as mobile phone, global positioning systems (GPS), and computers in our daily life, finding one alternative clean, sustainable power electrical supply becomes more and more important. The idea of harvesting energy from human motion is based on the fact that the average person's energy expenditure is 1.07e7 J per day, an amount equals to around 2500 mAh batteries [1], but the mechanical efficiency of the human body is estimated to be 15-30% [2], which means that most of the energy human consumed has been wasted into ambient environment. Even if we could only capture and recover small fraction of these wasted energy, there would be a significant economic and environmental impact to the society, especially for model military. Since 1990s, many researchers have brought up a lot of innovative ideas about energy harvesting from human motion. For example, shoe harvester from heel strike motion [3], knee energy harvester by generating energy when knee joint performed positive muscle work during walking [4], and suspended load backpack energy harvester [5].

All these three leading energy harvesting prototypes have been broadly developed, the most widely used and commercialized prototype nowadays is the suspended-load backpack energy harvester. Suspended load was first introduced in the Journal Science back in 2005 [5]. It converted mechanical energy from the vertical relative movement between human body and suspended backpack with carried loads to electricity during normal walking. The suspended-load backpack can generate up to 7.4W, and the heavier load you carried, the larger power output you can get. However, the only drawback to the suspended-load backpack is that little extra human metabolic cost is needed compared with rigid attached backpack.

Even though the prototype of this suspended-load backpack has been through several generations since it was proposed, the latest version most commercialized one, Lightning Packs, it still has few shortcomings, like low efficiency caused by oscillation of generator output in two directions, and low reliability due to the backlash and impact force. Thus, a new generation backpack energy harvester is motivated to be developed.

1.2 Objectives of the Thesis

The objective of this thesis is to design, fabricate and analysis the MMR based backpack energy harvester and compare it with traditional backpack energy harvesters. We used two types of modeling for simulation of the results of harvesters with human dynamics. One is simple dual mass model, the other more is a bipedal walking with suspended load model. Experiments were conducted to verify the advantages of MMR based backpack energy harvester.

1.3 Literature Review

1.3.1 Energy harvesting from human body

The concept of energy harvesting can be concluded as the process by which waste energy from external source (solar power, thermal energy, wind energy, kinect energy, etc.) is captured, converted and stored. Human body contains enormous quantities of energy. An average person of 69kg with 15% body fat could store energy around 390MR. However, the person only consumes from 70, 000 to 1400, 000 calories per hour depending on activity, which is around 81W to 1630W [6]. Even though we could only harvest 1% energy of energy wasted, it would make a significant difference for industries development, such as wearable electronics, wireless sensor networks, etc.

The energy resources for energy harvesting from human body can be generally divided into two parts: kinetic energy and thermal energy. The two parts could further be expended as detailed activities like joint rotation, enforcement of body weight, vertical displacement of mass centers, breath, heat dissipation, elastic deformation of tissues and other attachments, etc. [6] [7] which is shown in Figure 1-1.

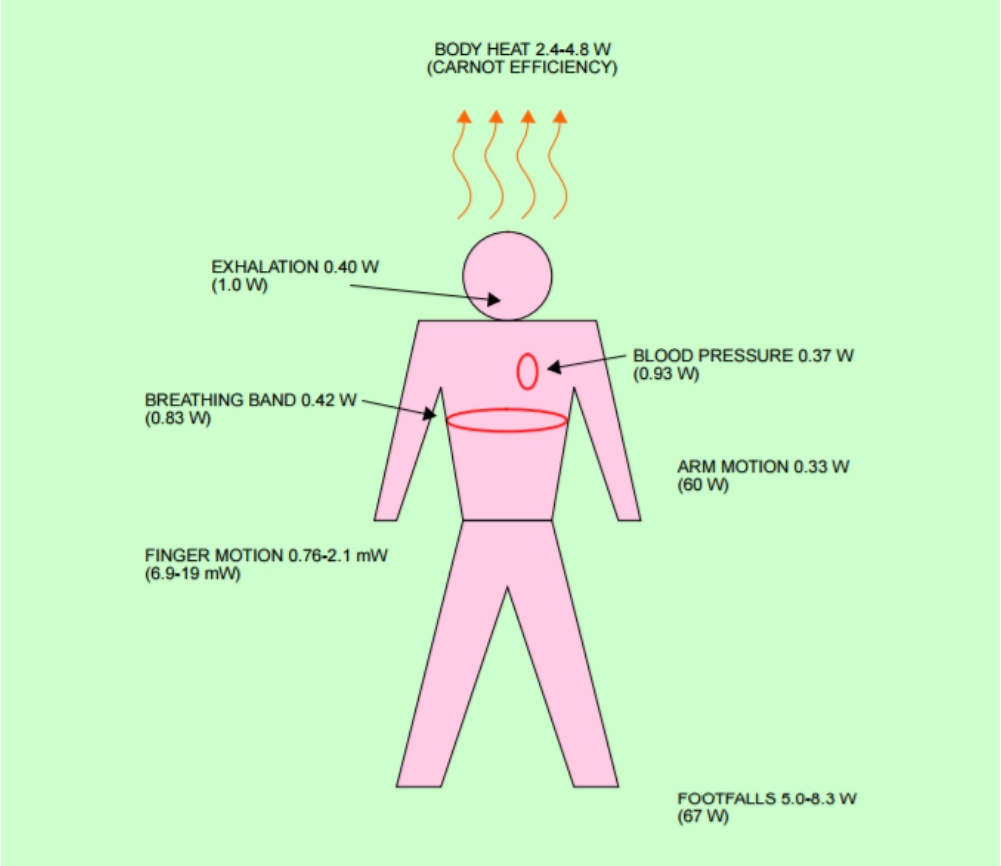

Figure 1-1 Available power sources from human body and their estimated power value in watts [6]. (Not all the available sources included)

Since the mechanical efficiency of human body is estimated to be about 15-30% [8], most of the energy human consumed is dissipated as heat. Thus, some novel thermoelectric and thermionic materials and some devices based on it has been designed and manufactured. The typical example of it is the Seiko Thermic wristwatch [7]. The wristwatch could generate sufficient energy, microwatts, from thermal gradient of bother heat over ambient temperature for clock movement. However, thermoelectric technology from human body has relatively low efficiency. For example, assuming an environmental temperature of 0°C, ZT=1, and a total sensible heat by a person walking at a natural speed is 100W, the maximum power available during walking would be approximately 2W [9]. In recent few decades, researchers have explore more on harvesting energy from the body motion, which may have much larger conversion efficiency than thermoelectric technology. Human walking has brought into people's sight since it is the most natural activity

that human perform every day and it involves a variety range of motions between different body segments.

1.3.2 Human walking

Walking, one of the most energy- consuming activities, is much more complicated than people normally thought. We adapt ourselves to different walking situations [10] and naturally change walking gait to lower expenditure form, such as by changing step length [11], different arm motion [12], etc. During walking, there is at least one foot always in contact with the ground, while for running, there is one phase that neither foot is contact with the ground [13]. There are some definitions of terms we will mention in next few chapters about human gait. Part of the terms have been demonstrated in Figure 1-2. We concluded as bellows [13] [14]:

1) Step length: The distance from heel strike of one foot is in contact with the ground to heal strike the foot occurs.
2) Stride length: The distance from heel strike of one foot to the next heel strike of the same foot happens again.
3) Stance phase: The period of time when a given foot is in contact with the ground. It starts from heel strike of the foot and end with the toe off of the same foot.
4) Swing phase: The period of time when a foot is not in contact with the ground. It starts from the foot's toe off, and it continues when the foot swings forward, at last it ends with the foot's heel strike.
5) Single support: The period of time in a complete gait when only one foot is in contact with the ground.
6) Double support: The period of time in a complete gait when both feet are in contact with the ground at the same time.
7) Ground Reaction Force (GRF): The force exerted on the foot by the ground.

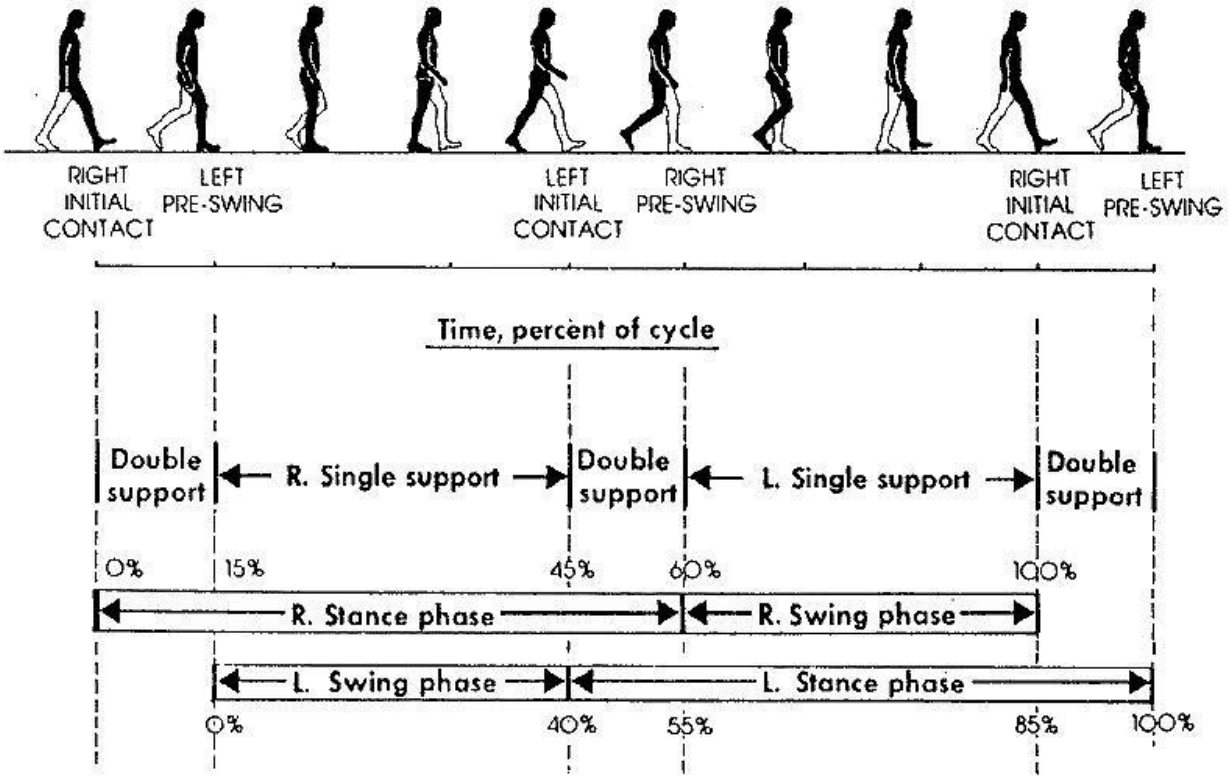

Figure 1-2 Terminology to describe the events of the gait cycle [15]

1.3.3 State of art energy harvesters from human motion

Heel strike

Heel strike refers to the point when the forward limb makes contact with the ground. Riemer et al. [9] calculated potential power available from heal strike based on assumption that the maximum GRF acted on the shoe is around 1.2 times of the body weight. A body weight of 80kg, with a 4mm displacement during heel strike. The theoretical maximal power will be 4W. Figure 1-3 shows two of the earliest design of shoe energy harvesters from MIT Media Lab [16]. The shoe in Figure 1-3 (a) harvested energy from flattening by piezoelectric material (PZT) at the heel and from toe off event by bending a bimorph stave [7]. The average power harvested is 8.3 mW at the heel and 1.3 mW at the toes during a standard walking. By embedded generator inside the sneaker as Figure 1-3 (b), 60 mW of average power could be generated [16]. In recent years, Xie et al. [17] brought up the idea of motion magnification for human foot strike, sliding mechanism as shown in Figure 1-4, with approximately 1 W power output during normal walking. However, for current state of art technology with piezoelectric transducers or similar piezoelectric cells to generate

electrical energy from pavement, the output was limited to within 100mW with each PZT transducer [18].

(a) (b)

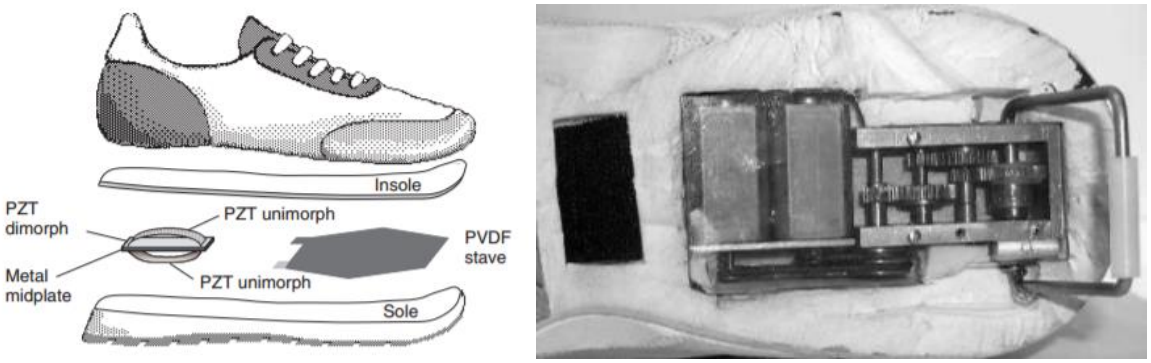

Figure 1-3 Two types of shoe energy harvesters from MIT Media Lab [16]: (a) integration of a 31-mode piezoelectric dimorph under the heel and a PBDF stave under the ball of the foot; (b) A twin motor-generators and step-up gears embedded in a sneaker's sole.

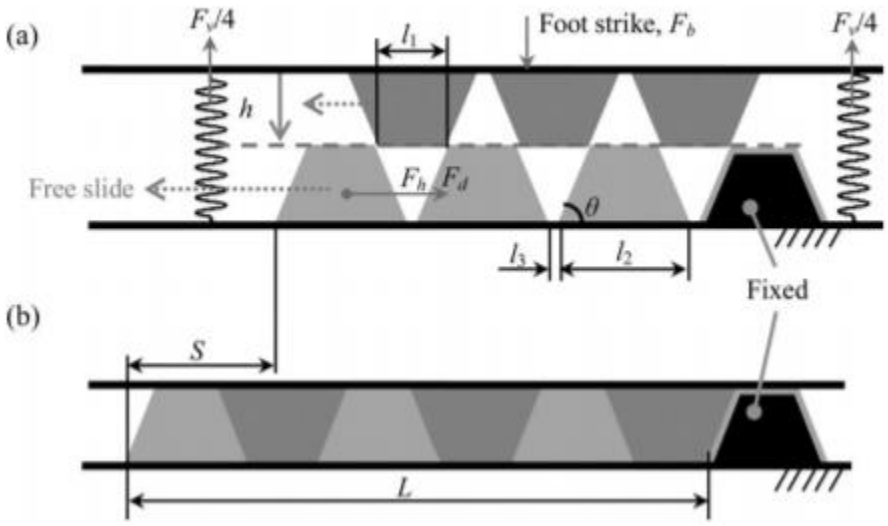

Figure 1-4 Sliding mechanism with force analysis [17]: (a) fully released; (b) fully pressed.

Knee

In all the motions during walking, muscles generates torque at the joints. Winter et al. defined positive work, the work performed when the muscle moment is in the same direction as the angular velocity of the joint, and negative work as muscle moment is in the opposite direction of the

angular velocity of the joint [8]. Researchers mostly focused on negative work phase since metabolic cost is expected to be reduced during negative work phase. Knee energy harvester has been investigated a lot since it largest portion of negative work compared with hip and ankle according to researchers' calculation [9].

The one of state of art knee energy harvester is the one from Donelan et al.'s study [4] as shown in Figure 1-5. Researchers compared two modes: continuous generation mode and generative braking mode [4]. The continuous mode harvested energy continuously, while generative braking mode only harvested energy during negative work phase. The generated braking model could generate average 4.8 W with a litter more metabolic power around 5 W and in continuous generation mode could generate 7.0 W with 18W more metabolic power [4]. One of other state of art shoe energy harvester is a magnetically plucked wearable knee-joint energy harvester (Mag-WKEH) as shown in Figure 1-6 [19]. The working principle Mag-MKEH is that the piezoelectric bimorph is excited by the primary magnets (PM) no matter what walking frequency is. This device could achieve high energy output of 1.9 mW to 4.5 mW depending on walking speed [19].

(a) (b)

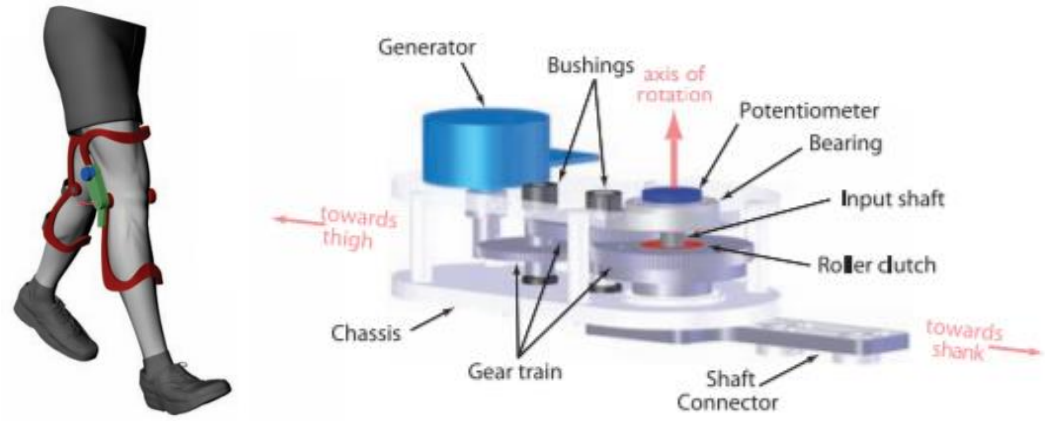

Figure 1-5 Biomechanical energy harvester [4]: (a) two harvesters worn on each leg; (b) the chassis contains a gear train with a one-way clutch that allows engagement at knee extension and disengagement at knee flexion.

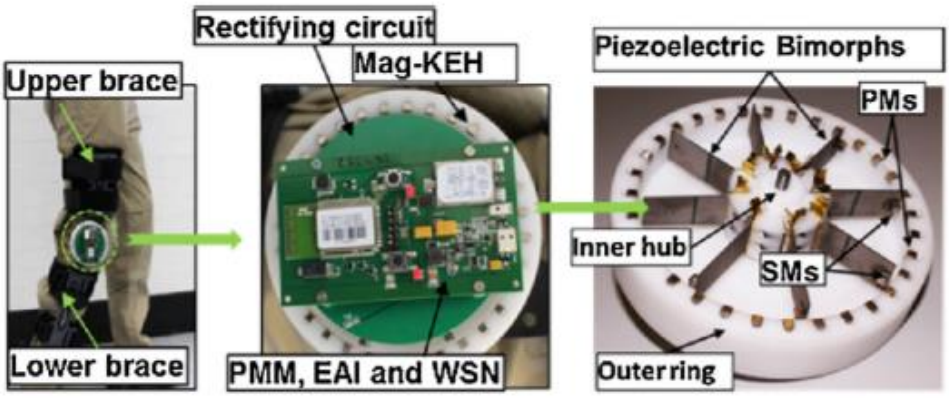

Figure 1-6 Prototype of the piezoelectric knee-joint energy harvester, Mag-WKEH [19].

Center of mass motion

The center of mass motion of human during walking is similar to a 3-D wave [9], like vertical displacement and lateral displacement. The peak to peak of the vertical COM motion is approximately 5 cm [2]. According to estimation from Riemer et al.'s study [9], a potential power of 20 W for a 5 cm vertical COM motion with a 20 kg device. In last ten years, a lot of researchers have begun to look into obtaining electricity from the relative movement between human and backpack during walking. The device we used to magnify the relative displacement is called suspended load backpack. The state of art in backpack energy harvesting is suspended load backpack energy harvester like shown in Figure 1-7 [5], which could generate 7.4 W at a fast waling speed. The additional metabolic cost is less than 40 % of that required by traditional human power generation, such as hand-crank generators, wind-up flashlights, etc. [9].

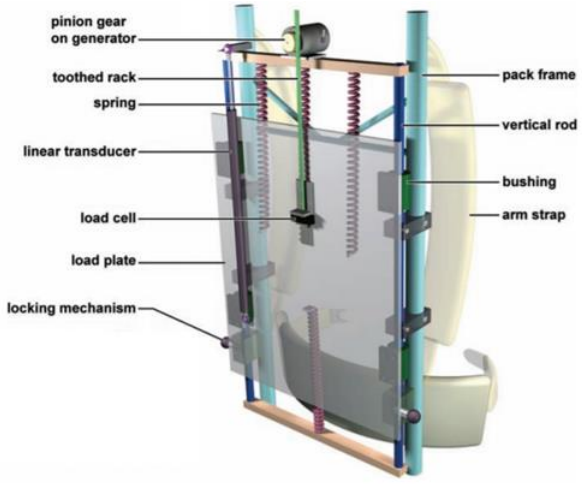

Figure 1-7 The suspended load backpack energy harvester [5].

While generating electricity, the device could decrease backpack load exerted to the human body during high energy expenditure period, when walking with properly phased motion between backpack and harvester [5] [20] [21] [22]. It could also reduce the peak force on human body with an elastically-suspended backpack compared with a rigid attached backpack [5] [23] [24]. Since the great power potential and advantages of backpack energy harvester, it motivates us to look further into it and will explain in detail in next few chapters.

Design criteria for energy harvesting from human motion

The criteria for designing new generation of energy harvester scavenged from human motion are concluded as follows:

1) Light weight
2) Could be easily implemented on the person.
3) High power output and high energy conversion efficiency.
4) High reliability.
5) Low extra metabolic cost.
6) Comfort feeling for wearer.
7) Will cause a difference in human natural walking gait as little as possible.

1.4 Contributions of the Thesis

The research accomplished in this thesis includes:

1) A mechanical motion rectifier (MMR) based power takeoff system, a new generation of backpack energy harvester, with high efficiency, high reliability and broad bandwidth has been designed, fabricated and analyzed.

2) One dual mass system models are used to compare three types of harvester, pure damping, traditional, and MMR based backpack energy harvester, and to study the effect of different tuning and damping ratios on the power output, human peak forces and human metabolic cost.

3) To better explain basic physics of human walking, like COM motion, GRF etc., a bipedal walking with suspended backpack model has been developed to compare traditional

energy harvester and MMR based backpack energy harvester. The limitations and future work of this bipedal walking model have also been discussed in this thesis.

4) Experiments conducted for verifying that MMR based backpack energy harvester has larger power output than traditional backpack energy harvesters and other advantages over traditional energy harvester, like high efficiency and high reliability. Up to 4.84W average power could be reached by MMR based backpack energy harvester when the subject walking at 3.5mph on the treadmill.

1.5 Thesis Organization

The thesis is organized as follows. The motivation, objective, and contribution has been presented in Chapter 1. Chapter 2 introduces the concept, modeling, design and fabrication of MMR based backpack energy harvester. Chapter 3 compares traditional backpack energy harvesters with MMR based backpack energy harvester via a simple dual mass model. The optimal parameters for harvester power output or best 'Human Harvester Efficiency' point, which is also introduced. The advantages and limitations of dual mass model discusses the last subchapter in Chapter 3. In Chapter 4, a bipedal walking with suspended load model, a bipedal walking model, has been introduced for better mimicking behaviors of human walking. The stability, optimal parameters for power output and limitations are studied in Chapter 4. Traditional harvesters and MMR based backpack energy harvester are compared again with the new bipedal model in Chapter 4. The frequency content of different COM motion has also been studied in Chapter 4. Experiments conducted to verified that MMR based backpack energy harvester has larger power output than traditional backpack energy harvesters and other advantages, are demonstrated in Chapter 5. Chapter 6 concludes the content of this thesis and gives recommendations for future work.

2. MMR based backpack energy harvester

2.1 Chapter Introduction

This chapter introduces the concept, modeling, design and manufacturing of MMR based backpack energy harvester. The objective of the proposed research is to investigate and design a new generation of backpack energy harvester with high efficiency, high reliability and broad bandwidth performance energy harvester. MMR energy harvester was first introduced in energy-harvesting shock absorber in 2012 [25]. The regenerative shock absorbers proposed in [25] can significant improve the energy harvester efficiency, achieved over 60 % efficiency at relative high frequency range which is much higher than conventional regenerative shock absorbers, reduces impact forces and harvests high power output, more than 15 W at when driving test vehicle at 15 mph. At the same time. Literature reviews about advantages of MMR based energy harvester compared with traditional energy harvester is discussed in detail later in Chapter 2.2. Since first introduced MMR based regenerative shock absorbers, MMR mechanism has been implanted in several other energy harvesting projects, like railway energy harvester, ocean wave energy harvester, wildlife tracking etc. [26] [27] [28]. We also introduces the parameters for the MMR based backpack energy harvester we proposed. One degree of freedom (dof) model simulation results for the MMR based backpack harvesters is presented as well.

2.2 The concept of Mechanical Motion Rectifier mechanism

The innovative concept of 'mechanical motion rectifier' is to convert bidirectional motion into unidirectional motion, which cannot be simply replaced by an electrical voltage rectifier. They key components of the mechanical motion rectifier are normally two one way clutches which could transmit one direction rotation to the motor. As shown in Figure 2-1, assuming the input is first upward, only the left blue one way clutch is engaged with the shaft while the right one is in disengaged status, the shaft is in clockwise rotation. The shaft is connected with gearbox and generator via a shaft coupling. However, when the input is downward, the red one way clutch is in engagement while the blue one is in disengagement. In this case, the shaft only rotates clockwise direction. Certainly, the blue one way clutch engagement period to the next red one way clutch engagement period is not continuously. There is one 'gap' between two engagement and the shaft at that time is freely rotated with gearbox and generator, we called this 'gap' period disengage period or disengagement.

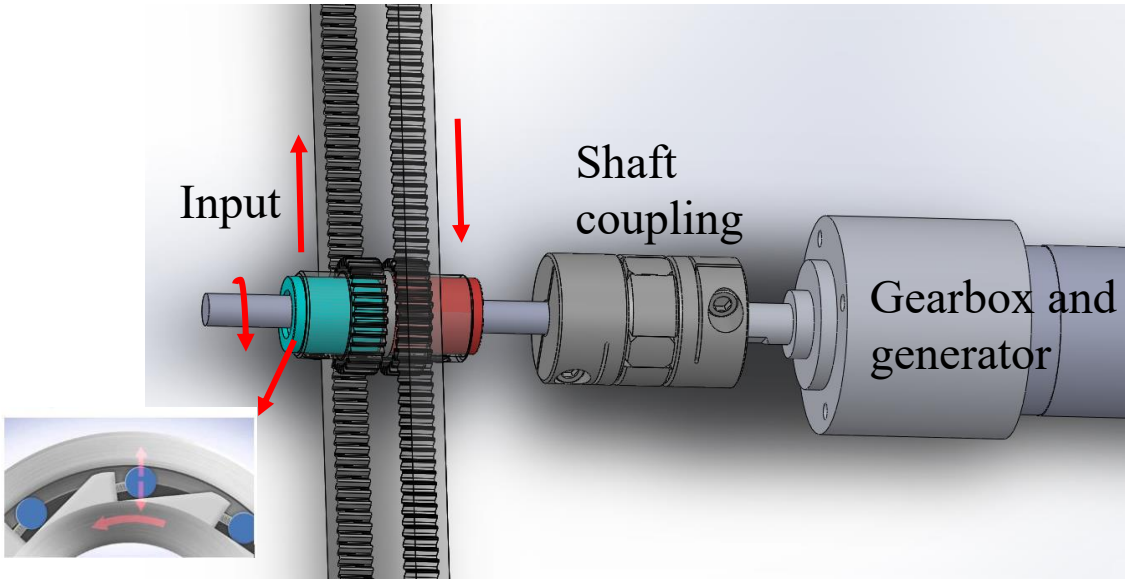

Figure 2-1 Concept of Mechanical Motion Rectifier.

Unlike a full- wave voltage rectifier, normally with motion rectifier, the voltage output will not drop to zero as shown in Figure 2-2 (b) blue line represents motion rectifier output result. However, when input frequency is very low, it will make the result of Motion rectified energy harvester similar as one traditional energy harvester since disengage period disappears. But with a voltage rectifier, it only functions as an 'absolute value' in Mathematics like pink line in Figure 2-2 (b).

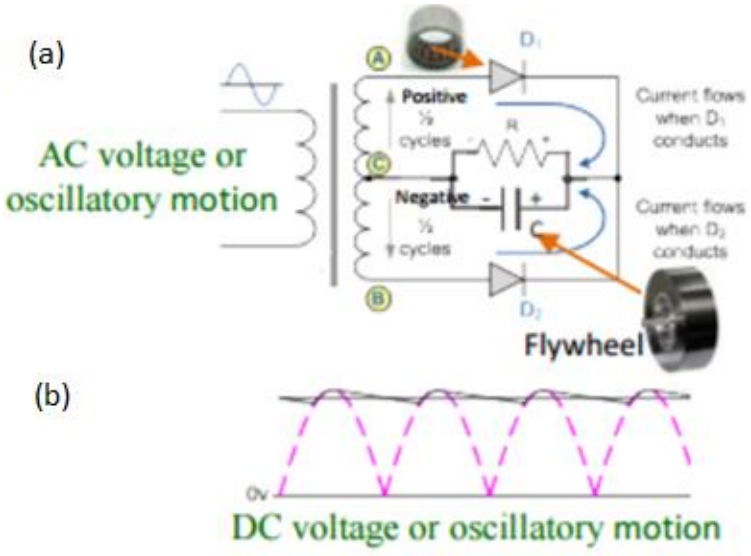

Figure 2-2 Electrical analogy for 'motion rectifier'[25]: (a) The mechanical motion rectifier with two roller clutches can be analogy to a full-wave voltage rectifier using a center-tapped transformer and two diodes; (b) motion rectifier result compared with electrical rectifier.

For typical vibration based energy harvesters, they normally used rack pinion transmission system to input signals into the system. While there are still some innovative energy harvesters used ball screw. Here, we only discussed about rack pinion based energy harvester. The unidirectional rotation decreases impact force, reduce backlash and friction in the transmission system compared with bidirectional rotation of conventional energy harvesters [25]. With traditional rack pinion transmission system, the rack teeth were worn out and broken quickly. Thus MMR based energy harvester has higher reliability compared with conventional rack pinion based energy harvesters. In addition, the bidirectional rotation generator output needs one additional electrical rectifier to power electronics or charge batteries.

2.3 Design and manufacture of MMR based backpack energy harvester system

2.3.1 MMR based backpack energy harvester

(a) (b)

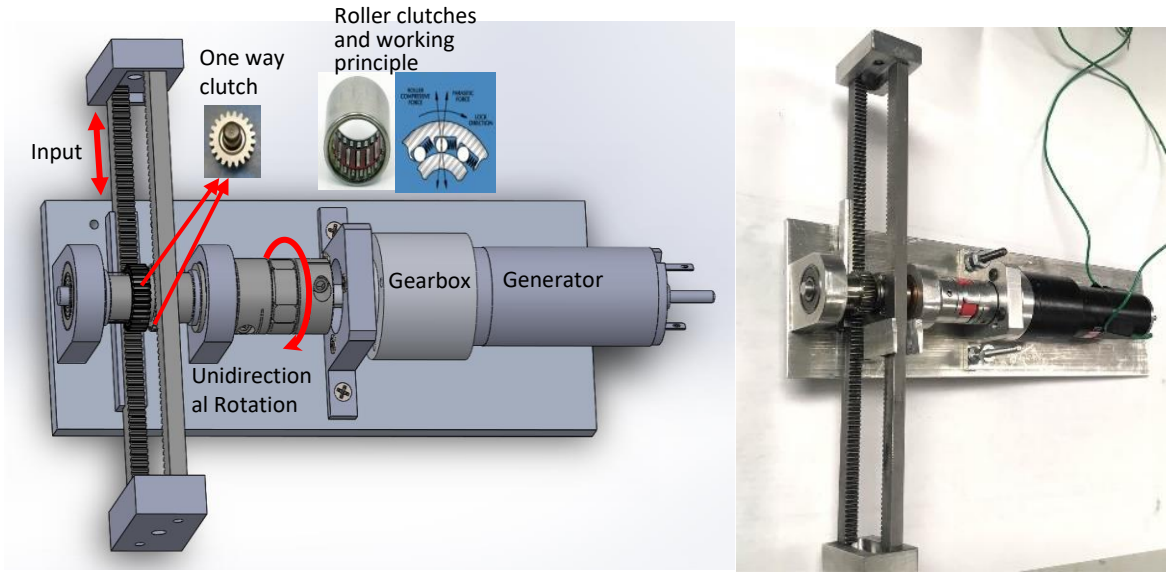

Figure 2-3 MMR based backpack energy harvester: (a) detailed design of MMR based backpack energy harvester; (b) assembled MMR based backpack energy harvester.

Figure 2-3 shows the detailed design and assembled MMR based backpack energy harvester. The first part of the MMR based energy harvester is the motion rectifier we have introduced in Chapter 2.2. It consist of two spur gears and each embedded with a one way clutch. We have a u channel as shown in Figure 2-3 (a) to guide the direction of the rack. However, in the assembled prototype as shown in Figure 2-3 (b), we have added another linear guide. To reduce friction between rack and u channel, we added grease between them. The second part of the MMR based backpack energy harvester is one 33:1 ratio gearbox and a generator. The function of the backboard is for the convenience of fixing the harvester with the suspended load frame we designed, which will be introduced in Chapter 2.3.2. The total weight of the harvester including the back board is less than 2 pounds.

2.3.2 Suspended load backpack frame

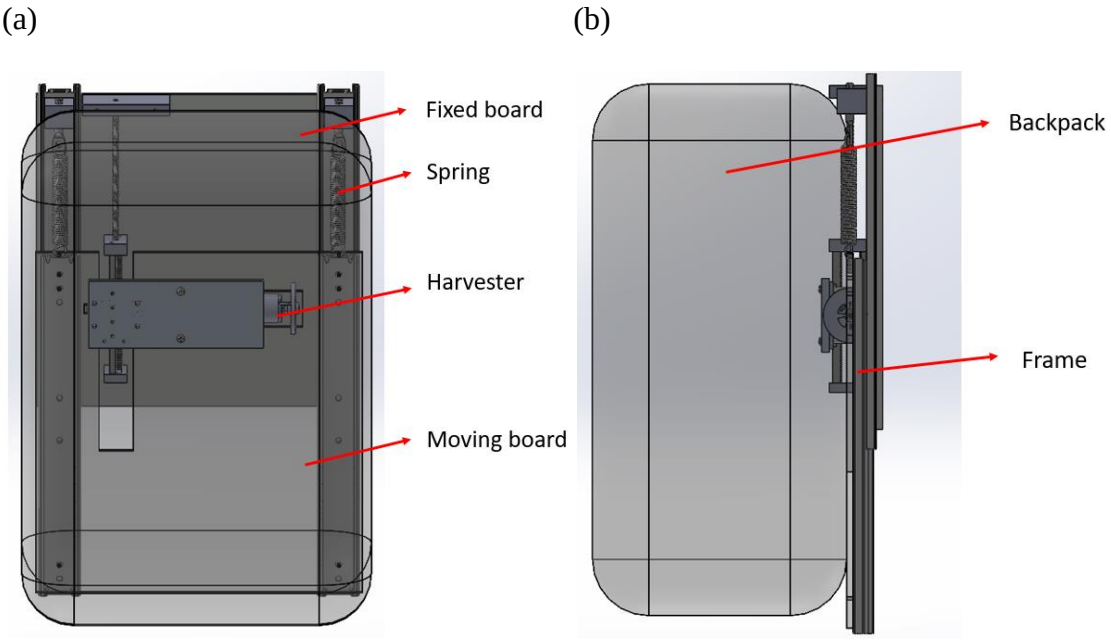

Figure 2-4 Design of suspended load backpack frame implemented with MMR based backpack energy harvester; (a) front view; (b) side view.

Figure 2-4 shows the design of suspended load backpack frame with implemented MMR based backpack energy harvester. The frame consists of two boards, a fixed board and moving board. The fixed board and moving board are connected by two 1079N/m (6.16 lbs./inch) extension springs and one rigid rod to attach two racks of the harvester with the fixed board. Assembled prototype is shown in Figure 2-4. The weight of metal block load on the moving board is depended on what parameters we choose to study and is discussed in Chapter 2.3. In order to lighten the weight of backpack frame, it was made of Delrin plastic material. One displacement sensor, one force sensor, and Coco-80 vibration data collector for experiment data collection of harvester voltage output and sensor output have been implemented for data measurement as shown in Figure 2-5. All the sensors and equipment used for experiments will be discussed in detail later in this thesis.

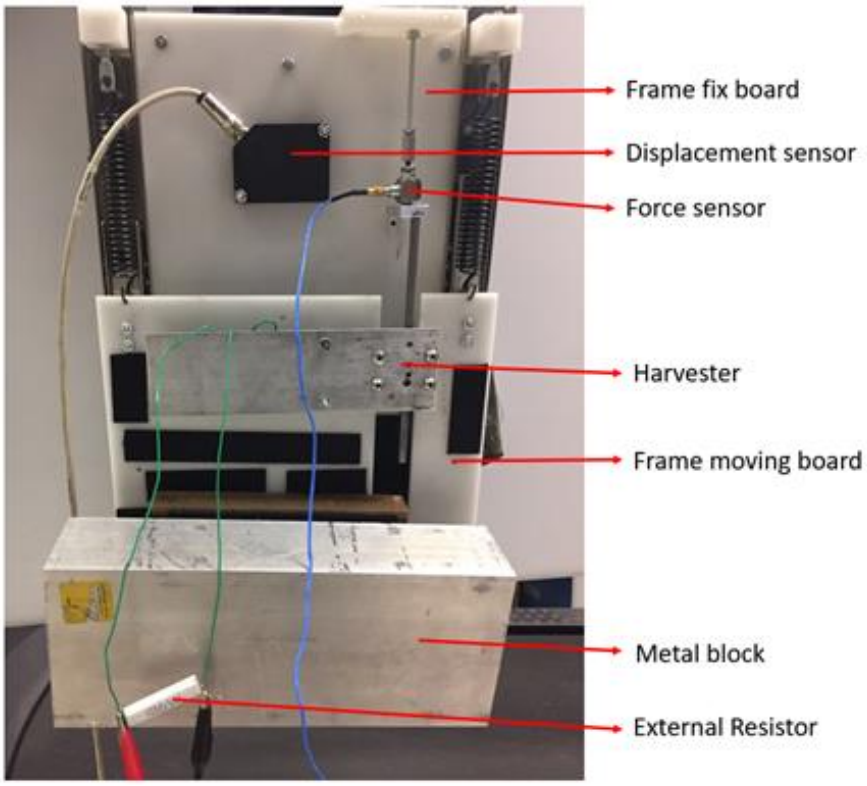

Figure2-5 Assembled suspended load backpack frame with MMR based backpack energy harvester.

2.3.3 Covert MMR based to traditional backpack energy harvester

To better understanding and study the MMR based backpack energy harvester, we will compare the MMR based backpack energy harvester with traditional rack pinion based energy harvester. In this case, it is better we could keep structure the same besides the motion rectifier part. As shown in Figure 2-6, to convert our MMR based backpack energy harvester to traditional rack pinion energy harvester, we only take one rack out and replace the spur gear we used in the MMR based

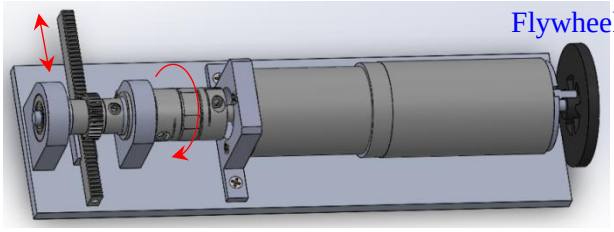

backpack energy harvester, which embedded a one way clutch with a regular same size spur gear.

Figure 2-6 Traditional backpack energy harvester converted from MMR based backpack energy harvester.

2.4 Modeling of MMR based backpack energy harvester

2.4.1 Target people group

Much research has been done on the elasticity of the backpack load, and its effect on the human body. It is becoming more and more apparent that elasticity of the suspended-load backpacks is useful for human walking cost. The suspended-load backpack could reduce the peak force and energy cost during locomotion [23].

For our project, our target population is military soldiers since it will benefit a lot for people who already needs to carry a heavy backpack. Back before the 18^{th} century, foot soldiers already started to carry over 15 kg lord while they marched [29]. Since then, the loads have progressively risen to up to 50 kg as shown in Figure 2-7 because of rapid technology development in variety types of weapons, protection, communication and other equipment. Normally, the heavier the load is, the larger power output the backpack harvester could generate. However, the heavier the load is, the more burden people who wears it might feel. We will not study the effect of different load to the harvester in this thesis. We use 15 kg as a fixed backpack load for the study. Currently, there have been several backpack energy harvesting been explored by US army, like Energy Harvesting Assault Pack (EHAP), which could generate more than 3 W at 3 mph as shown in Figure 2-8 (a) [30], Lightning Packs as shown in Figure 2-8 (b) [31].

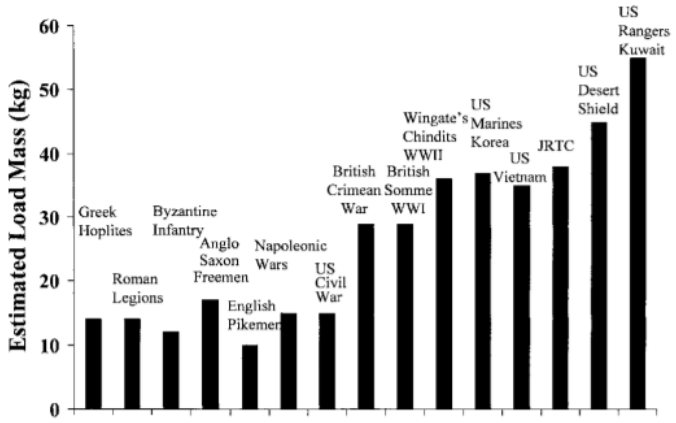

Figure 2-7 Loads carried on the march by various infantry units throughout history [29].

(a) (b)

Figure 2-8 Current backpack energy harvesting application for soldiers: (a) Energy Harvesting Assault Pack (EHAP) [30]; (b) Lightning Packs [31].

2.4.2 Modeling of MMR based backpack energy harvester

In Li et al.'s study [25], they analyzed the motion rectifier with differential equations and introduced the modeling of the system based on circuits as shown in Figure 2-9. This circuit based method could simulate the output voltage of the MMR based energy harvester. However, in this thesis, we modeled the system by using Lagrange Equation [32].

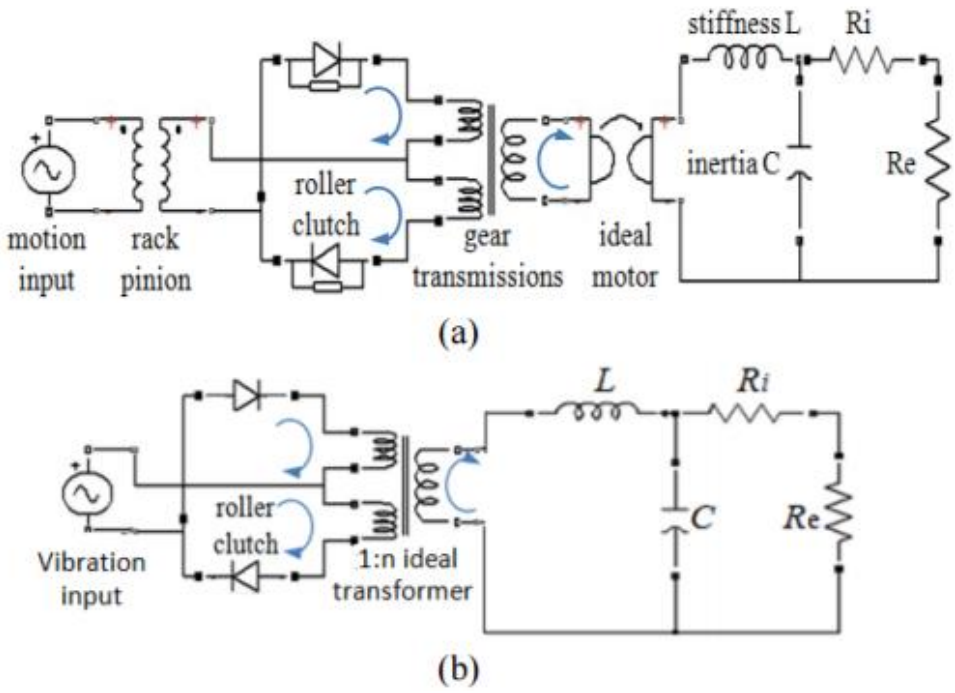

Figure 2-9 Modeling for regenerative shock absorber using electrical circuit [25]: (a) original, (b) simplified.

Lagrange equation for dynamic equation of MMR based energy harvester is

$$\frac{d}{dt}\left(\frac{\partial L}{\partial \dot{q}_i}\right)-\frac{\partial L}{\partial q_i}=Q_i \tag{2.1}$$

Where $L=T-V$. T and V are kinetic and potential energy of the system. The input displacement is x, which is chosen as the generalized coordinate of the system. Assuming that the system has an external driven force F . The kinetic energy of the system is

$$T=2\cdot\frac{1}{2}m_r\dot{x}^2+2\cdot\frac{1}{2}J_p\omega_p^2+2\cdot\frac{1}{2}J_c\omega_c^2+\frac{1}{2}J_s\omega_s^2+\frac{1}{2}J_{gb}\omega_{gb}^2+\frac{1}{2}J_{ge}\omega_{ge}^2 \tag{2.2}$$

Where m_r is the rack's mass, and J_p , J_c , J_s , J_{gb} and J_{ge} are the moment of inertia of the pinion, one way clutch, shaft, gearbox and the generator. Also, ω_p , ω_c , ω_s , ω_{gb} and ω_{ge} are the angular velocity of the pinion, one way clutch, gearbox and the generator. Since the pinion, one way clutch, shaft, gearbox are assembled on the same shaft which is driven by x , it has a relation that $\omega_p=\omega_c=\omega_s=\omega_{gb}=\frac{\dot{x}}{r}$, where r is the diameter of the pinion, and since rotational speed of

the generator speeds up by the gearbox $\omega_{ge} = n_g \frac{\dot{x}}{r}$, where n_g is the gear ratio of the gearbox. The potential energy in the system here is $V = 0$. When the MMR system is in the engagement, the generalized force Q is the result of external force F influenced by force from the generator. However, when the MMR system is in the disengagement, the generalized force Q is equal to external force F. The torque of the generator is proportional to the generated current I_{ge} with a torque constant k_t, while the voltage of the generator V_{ge} is proportional to angular speed ω_{ge} with a voltage constant k_e. So the generalized force Q to the coordinate x in engagement is

$$T_{ge} = k_t I_{ge} = \frac{k_t V_{ge}}{R_i + R_e} = \frac{k_t k_e \omega_{ge}}{R_i + R_e} = \frac{k_t k_e n_g \dot{x}}{(R_i + R_e) r} \tag{2.3}$$

$$Q = F - \frac{k_t k_e n_g^2 \dot{x}}{(R_i + R_e) r^2} \tag{2.4}$$

Where R_i and R_e are internal resistor of the generator and external resistor. The dynamic equation of the engaged system is the result of plugging in equation (2.2) and (2.4) into equation (2.1)

$$(2m_r + \frac{2J_p + 2J_c + J_s + J_{gb} + n_g^2 J_{ge}}{r^2})\ddot{x} = F - \frac{k_t k_e n_g^2 \dot{x}}{r^2 (R_i + R_e)}$$

$$(2m_r + \frac{2J_p + 2J_c + J_s + J_{gb} + n_g^2 J_{ge}}{r^2})\ddot{x} + \frac{k_t k_e n_g^2 \dot{x}}{r^2 (R_i + R_e)} = F \tag{2.5}$$

In this case, we could define equivalent mass and equivalent damping of MMR engaged system m_e and c_e as

$$\begin{cases} m_e = 2m_r + \dfrac{2J_p + 2J_c + J_s + J_{gb} + n_g^2 J_{ge}}{r^2} \\ c_e = \dfrac{k_t k_e n_g^2}{r^2 (R_i + R_e)} \end{cases} \tag{2.6}$$

In practical MMR system design, the total mass of two racks $2m_r$ is relatively small and can be ignored. In addition, J_c, J_s and J_{gb} are very small compared with $n_g^2 J_{ge}$. Thus, m_e and c_e in engagement period can be simplified as in equation (2.7)

$$\begin{cases} m_e \approx \dfrac{n_g^2 J_{ge}}{r^2} \\ c_e = \dfrac{k_t k_e n_g^2}{r^2 (R_i + R_e)} \end{cases} \tag{2.7}$$

While in disengage system, the MMR system can be divided into two parts. One is rack and pinion. The other one is consist of one way clutch, shaft, gearbox and the generator. The generalized force for the first part is $Q = F$ and the generalized force for the second part is $Q = -\dfrac{k_t k_e n_g^2 \dot{x}}{r^2 (R_i + R_e)}$. Two dynamics equations disengaged MMR system are

$$\begin{aligned} &(2m_r + \frac{2J_p}{r^2})\ddot{x} = F \\ &\frac{2J_c + J_s + J_{gb} + n_g^2 J_{ge}}{r^2}\ddot{x} + \frac{k_t k_e n_g^2 \dot{x}}{r^2 (R_i + R_e)} = 0 \end{aligned} \tag{2.8}$$

Based on equation (2.8), the angular velocity of the generator will decrease exponentially with a time constant τ.

$$\begin{aligned} &\omega_{ge} = \omega_{ge0} e^{-\frac{t}{\tau}} \\ &\tau = \frac{2J_c + J_s + J_{gb} + n_g^2 J_{ge}}{\dfrac{k_t k_e n_g^2 \dot{x}}{(R_i + R_e)}} = \frac{m_e}{c_e} \end{aligned} \tag{2.9}$$

Where t is the time moment when the disengagement happens.

2.4.3 One dof model, parameters and results of MMR based backpack harvester

(a) (b)

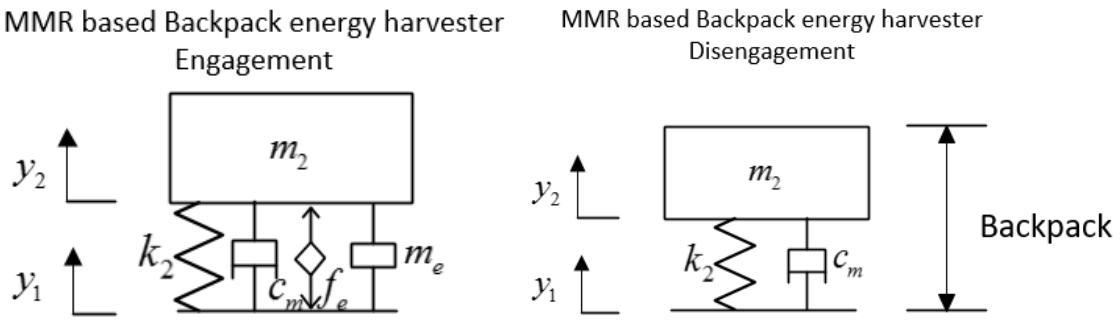

Figure 2-10 One dof model of MMR based backpack energy harvester. (a) engagement system; (b) disengagement system.

To demonstrate the results we got in Chapter 2.4.2, we are using a 1 dof model with our MMR based backpack energy harvester as shown in Figure 2-10. The left figure in Figure 2-10 represents a engaged MMR system in a 1 dof model with mechanical damping c_m caused from friction or anything other than equivalent damping from system, equavelent damping force f_e, equivalent mass from the system m_e and a spring k_2 for 1 dof model. While in the disengaged MMR system as shown in the right figure of Figure 2-10, the system only has the spring k_2 and mechanical damping c_m. The values of parameters are listed in Table 2.1.

Table 2-1 Parameters for 1 dof model

Backpack mass	m_2	15 kg
Spring constant	k_2	2000 N/m
Radius of pinion gear	r	$7.9375e^{-3}$ m
Mechanical damping	c_e	50 N-s/m
Moment of inertia of the generator	J_{ge}	$1.17e^{-6}$ kg-m^2
Gear ratio	n_g	33 to 1
Internal resistance of the motor	R_i	0.273 Ω
External resistance	R_e	2 Ω
Torque constant	k_t	$7.99e^{-3}$

Voltage constant	k_e	0.008
Base excitation	y_1	$0.05\sin(2\pi ft)$ m
Excitation frequency	f	2 Hz

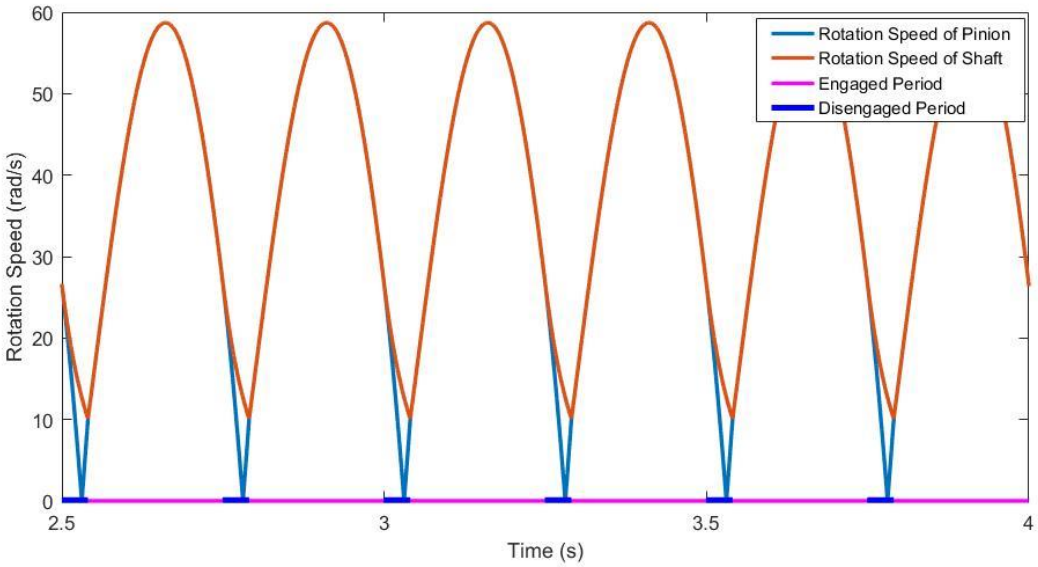

Figure 2-11 One dof Rotation speed result of MMR model.

The simulation result of 1 dof model shown in Figure 2-10 using MATLAB is shown in Figure 2-11. Fiugre 2-11 shows the comparison between input pinion speed and output shaft speed. It clearly shows the function of MMR system as a rectifier. The voltage output is proportional to the rotation speed of the shaft, which is the orange line, while the blue line represents the rotation speed of the input.

2.5 Chapter summary

In this chapter, the design and assembled prototype of our MMR based backpack energy harvester and the suspended load frame are presented. The concept of motion rectifier has been explained and we also compared it with electrical rectifier to show the advantages of our motion rectifier, which is not just a substitution of full-wave electrical rectifier. The model and two stage of MMR system solution, engagement and disengagement, has been illustrated and concluded as follows.

The engagement MMR system could be simplifier as equivalent mass m_e and equivalent damping c_e as shown in equation (2.7). The output of disengagement MMR system will decrease exponentially with a time constant τ from the moment disengagement happens as shown in equation (2.9).

In the last section of this chapter, we modeled and simulated a 1 dof model with MMR system with parameters we used to simulate our MMR based backpack energy harvester in Table 2-1. It will be used in next few chapters as well.

3. Compared with traditional energy harvester using a dual mass model

3.1 Chapter Introduction

This chapter compares MMR based backpack energy harvester and traditional backpack energy harvesters using a simple dual mass dynamics model. Three dual mass models for different distinct harvesters: pure viscous, non MMR, and MMR, are proposed, and a comparison in the output power and human comfort between the three models is discussed. As we mentioned before about energy harvesters from human motion design criteria, we need to consider human comfort and human effort since human will be wearing the harvesters and energy input of harvesters are human body itself. The concept of 'cost of harvesting' (COH) was first introduced by Donelan et al. in 2008 [4]. It is a dimensionless quantity defined for tradeoff between human metabolic cost and electrical power output of the harvesters. It defined as below.

$$COH = \frac{\triangle metabolicpower}{\triangle electricalpower} \tag{3.1}$$

Where $\triangle$ refers to the difference between walking while harvesting energy and walking while carrying the device but without harvesting energy [4]. In this chapter, we used a more straightforward term 'Human Harvester Efficiency' which $\triangle$ refers to difference between walking while harvesting energy and walking with load rigid attached. The optimal parameters for harvester power output and best 'Human Harvester Efficiency' point, which is also introduced. The advantages and limitations of dual mass model are discussed in Chapter 3.

3.2 Human walking dual mass model without energy harvester (Determining parameters)

Many human activities involve vibration in different forms, like eardrums vibrate to let us hear, the vibration of the light waves to let us see, and lungs vibrates for the human needs of breathing. Walking involves periodic motion of legs and trunk as well. In this case, we simulate human walking with backpack as a two degree-of-freedom (dof) system with base excitation, as shown in Figure 3-1 (a). The model doesn't include a flight phase during human walking, but only double support phase. The purpose of based excitation in the system is to adequately simulate the center of mass (COM) motion of human body during walking rather than attempting to describe the motion which occurs when the footsteps on the ground. Similar models have been extensively studied in other areas, however, our model is used to investigate the effect of k_2, harvester damping on harvester power output and human comfort.

The equation of motion for this system is shown as follows. We counts x from its static equilibrium position.

$$\begin{bmatrix} m_1 & 0 \\ 0 & m_2 \end{bmatrix}\begin{pmatrix} \ddot{x}_1 \\ \ddot{x}_2 \end{pmatrix}+\begin{bmatrix} c_1 & 0 \\ 0 & 0 \end{bmatrix}\begin{pmatrix} \dot{x}_1 \\ \dot{x}_2 \end{pmatrix}+\begin{bmatrix} k_1+k_2 & -k_2 \\ -k_2 & k_2 \end{bmatrix}\begin{pmatrix} x_1 \\ x_2 \end{pmatrix}=\begin{bmatrix} k_1x_0+c_1\dot{x}_0 \\ 0 \end{bmatrix} \tag{3.2}$$

The selection for parameters in the system is based on the following situation. When several male volunteers with average weight 76.8kg and average height 181.2cm walking with 15kg rigid-attached backpack under fast marching speed (average speed is 1.5m/s, average stride time is 1.067s), average peak to peak amplitude of COM motion is 0.05m [34]. According to Paolo de Leva and other researchers' study [32] [33], the male leg (femur and tibia) length when standing still is 43.4% of total body height, which is 0.79m in our model. In this case, base excitation of the system can be written as

$$x_0 = 0.79 + A * \sin(\frac{2\pi}{1.067/2}t) \tag{3.3}$$

The effective leg stiffness (k_1) equals 28000 N/m and effective leg damping (b_1) is 950 Ns/m [34]. To set A value, we need to simulate the x_1 using Matlab with $k_2 = \infty$, which means the backpack is rigid attached to the human body. As shown in Figure 5 (b), when $A = 0.0162$, the peak to peak x_1 value is 0.0503m. So x_0 is:

$$x_0 = 0.79 + 0.0162 * \sin(\frac{2\pi}{1.067/2} t) \quad (3.4)$$

(a) (b)

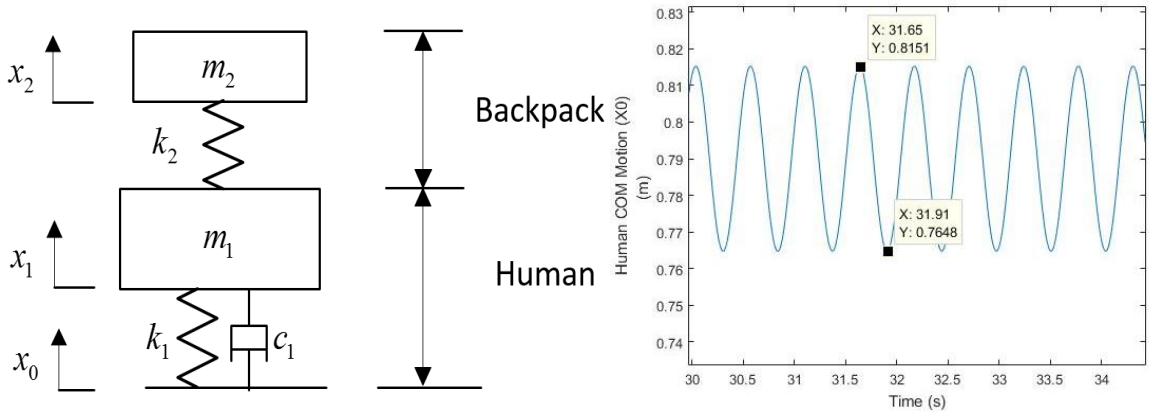

Figure 3-1 Dual mass model without harvester: (a) two mass system with base excitation model for human body with elastically attached backpack; (b) when the backpack rigid attached to human body, Center of Mass (COM) vertical displacement with set parameters during steady - state is 0.0503m when A=0.0162.

3.3 Energy harvester model with pure damping force

For the non-rotational vibration energy harvester, like piezoelectric harvester, the system can be modeled as Figure 3-2, where f_e is the equivalent force due to energy harvesting from equivalent damping c_e, and c_m is the mechanical damping coefficient. Thus, the total damping of the system $c_2 = c_m + c_e$.

The governing equations of the dual-mass vibration energy harvesting under base motion excitation can be written as:

$$\begin{bmatrix} m_1 & 0 \\ 0 & m_2 \end{bmatrix} \begin{bmatrix} \ddot{x}_1 \\ \ddot{x}_2 \end{bmatrix} + \begin{bmatrix} c_1 + c_m + c_e & -c_m - c_e \\ -c_m - c_e & c_m + c_e \end{bmatrix} \begin{bmatrix} \dot{x}_1 \\ \dot{x}_2 \end{bmatrix} + \begin{bmatrix} k_1 + k_2 & -k_2 \\ -k_2 & k_2 \end{bmatrix} \begin{bmatrix} x_1 \\ x_2 \end{bmatrix} = \begin{bmatrix} k_1 x_0 + c_1 \dot{x}_0 \\ 0 \end{bmatrix} \quad (3.5)$$

Where $c_e = \frac{k_t k_e {n_g}^2}{(R_i + R_e) r^2}$ which we defined before, k_t, k_e are the torque constant and speed constant, R_e , R_i are external resistance and the internal resistance. We can adjust R_e to control the value of c_e. And $f_e = c_e(\dot{x}_2 - \dot{x}_1)$. Since the motion excitation x_0 is harmonic, the system response will come to steady-state, which is in the form of:

$$x_2 - x_1 = (X_1 - X_2)\sin(\omega t - \theta) \tag{3.6}$$

Where the close form solution is

$$X_1 - X_2 = \frac{\sqrt{\omega^4 m_2^2 k_1^2 X_0^2 + \omega^6 m_2^2 c_1^2 X_0^2}}{\sqrt{\begin{matrix}(\omega^4 m_1 m_2 - \omega^2 m_2 k_1 - \omega^2 m_2 k_2 - \omega^2 m_1 k_2 - \omega^2 c_2 c_1 + k_1 k_2)^2 \\ +(\omega^3 m_2 c_1 + \omega^3 m_2 c_2 + \omega^3 m_1 c_2 - \omega c_1 k_2 - \omega c_2 k_1)^2\end{matrix}}} \tag{3.7}$$

Hence, the average power is:

$$\bar{P}_{ave} = \frac{1}{2} c_e \omega^2 (X_1 - X_2)^2 \tag{3.8}$$

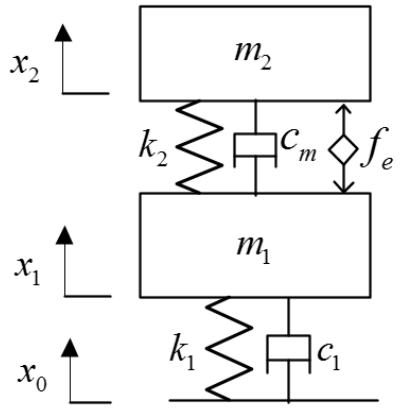

Figure 3-2 Dual mass vibration energy harvester model with equivalent damping force f_e.

Figure 3-3 (a) shows the average power output at different tuning ratio f $\left(f = \frac{\omega_2}{\omega_1}\right)$ and damping ratio ζ_e ($\zeta_e = \frac{c_e}{2m_2\omega_2}$), when $\zeta_m = \frac{c_m}{2m_2 w_2} = 1\%$ and its corresponding contours in the

Figure 3-3 (b), where $\omega_i = \sqrt{k_i / m_i}\,(i = 1, 2)$. As shown in these two figures, only one maximum power point exists, and it can reach to 23.73W when $f = 0.6$ and $\zeta_e = 0.04$.

(a) (b)

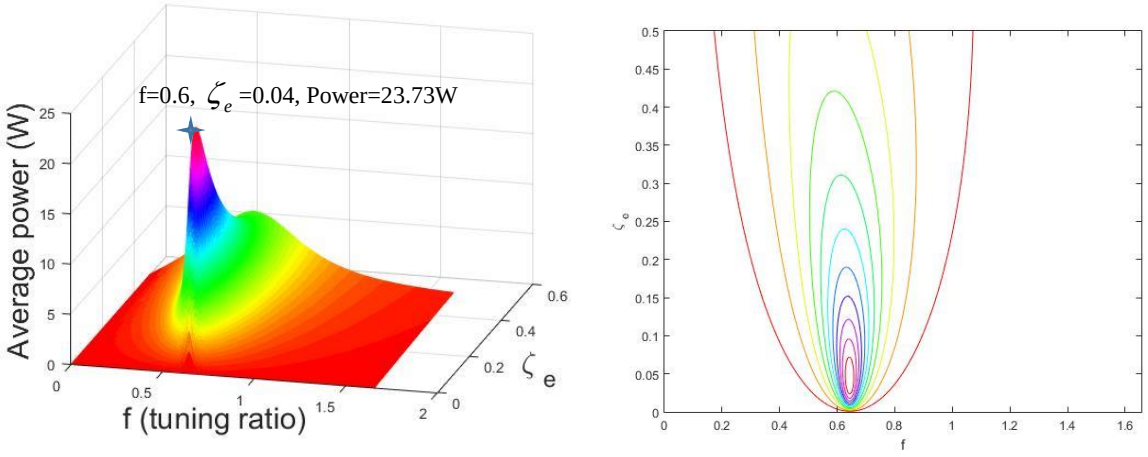

Figure 3-3 (a) average power at different tuning ratio and equivalent damping ratio ζ_e, where the mechanical damping $\zeta_m = 1\%$; (b) contours of average power at different tuning ratio and equivalent damping ratio.

(a) (b)

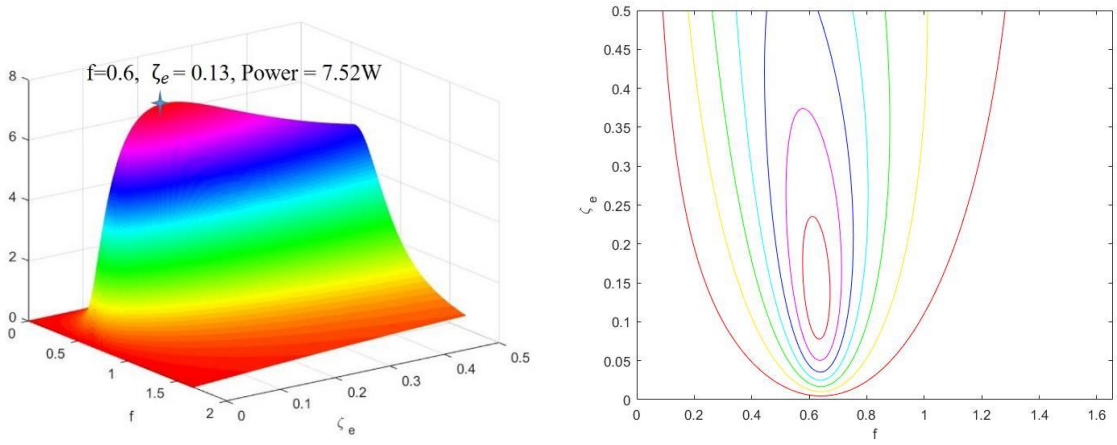

Figure 3-4 (a) average power at different tuning ratio and equivalent damping ratio ζ_e, where the mechanical damping $\zeta_m = 10\%$; (b) contours of average power at different tuning ratio and equivalent damping ratio.

However, when we increase the system mechanical damping ratio ζ_m to 10%, the optimal power will occur at different electrical damping ratio while ζ_e = 0.08, but at the same tuning ratio as when the system mechanical damping ratio is 1% as shown in Figure 3-3 (a). Figure 3-4 has also shown that system mechanical damping ratio will significantly influence the optimal power output value. The optimal power output for 10% mechanical damping ratio can only reach to 12.08W while with 1% mechanical damping ratio it can reach to 23.73W.

3.4 Traditional energy harvester model (Non MMR energy harvester)

For traditional energy harvester with generator or flywheel, an equivalent inertia will exist in the system and will be placed between m_1 and m_2 like in Figure 3-5.

The governing equations of the non MMR energy harvesting under base motion excitation can be written as:

$$\begin{bmatrix} m_1+m_e & -m_e \\ -m_e & m_2+m_e \end{bmatrix}\begin{bmatrix} \ddot{x}_1 \\ \ddot{x}_2 \end{bmatrix} + \begin{bmatrix} c_1+c_m+c_e & -c_m-c_e \\ -c_m-c_e & c_m+c_e \end{bmatrix}\begin{bmatrix} \dot{x}_1 \\ \dot{x}_2 \end{bmatrix} + \begin{bmatrix} k_1+k_2 & -k_2 \\ -k_2 & k_2 \end{bmatrix}\begin{bmatrix} x_1 \\ x_2 \end{bmatrix} = \begin{bmatrix} k_1x_0+c_1\dot{x}_0 \\ 0 \end{bmatrix} \quad (3.9)$$

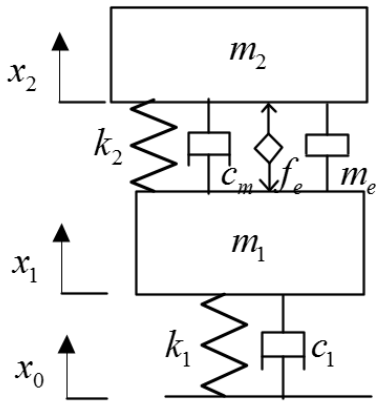

Figure 3-5 Dual mass vibration energy harvester model with equivalent damping force f_e and rotational inertia m_e.

Similarly,

$$X_1 - X_2 = \frac{\sqrt{\omega^4 m_2^2 k_1^2 X_0^2 + \omega^6 m_2^2 c_1^2 X_0^2}}{\sqrt{\begin{array}{l}(\omega^4 m_1 m_2 + \omega^4 m_1 m_e + \omega^4 m_2 m_e - \omega^2 m_2 k_1 - \omega^2 m_2 k_2 - \omega^2 m_1 k_2 - \omega^2 m_e k_1 - \omega^2 c_2 c_1 + k_1 k_2)^2 \\ +(\omega^3 m_2 c_1 + \omega^3 m_2 c_2 + \omega^3 m_e c_1 + \omega^3 m_1 c_2 - \omega c_1 k_2 - \omega c_2 k_1)^2\end{array}}} \quad (3.10)$$

And average power can be expressed as:

$$\bar{P}_{ave} = \frac{1}{2} c_e \omega^2 (X_1 - X_2)^2 \quad (3.11)$$

As shown in Figure 3-6, in the case of traditional non MMR harvester model, only one maximum point exists, but at different point compared to pure viscous damping force case in Chapter 3.3. The maximum power is 21.18W when $f = 0.96$ and $\zeta_e = 0.03$. Compared with Figure 3-7 when system mechanical damping ratio is 10%, similar conclusion could be made as pure damping model case when compared system mechanical damping ratio 1% with 10% that, the optimal power value will significantly decrease when higher mechanical damping is in the system. In addition, optimal power value can be reached when different electrical damping ratio ζ_e = 0.076 while the tuning ratio is the same as 1% mechanical damping ratio case.

(a) (b)

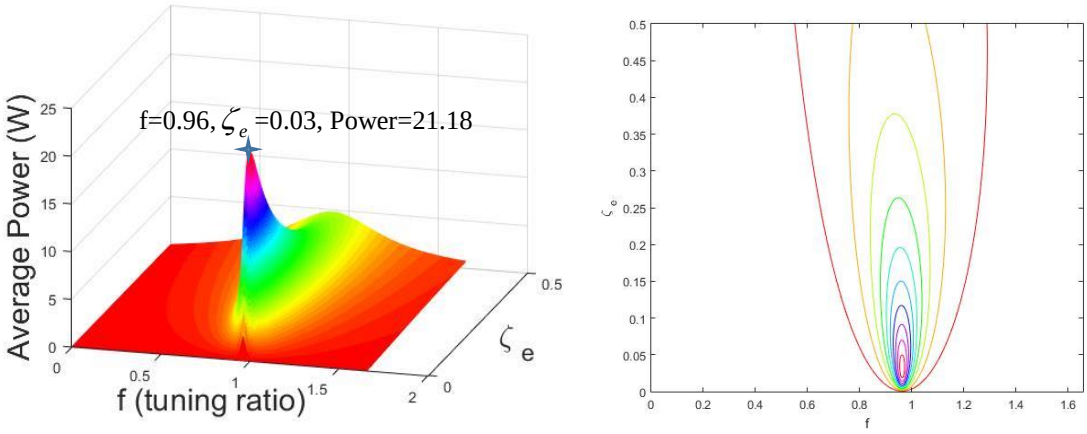

Figure 3-6 Traditional energy harvester result with dual mass model (a) average power at different tuning ratio and equivalent damping ratio ζ_e*, where the mechanical damping* ζ_m =1%. *(b) Contours of average power at different tuning ratio and equivalent damping ratio.*

(a) (b)

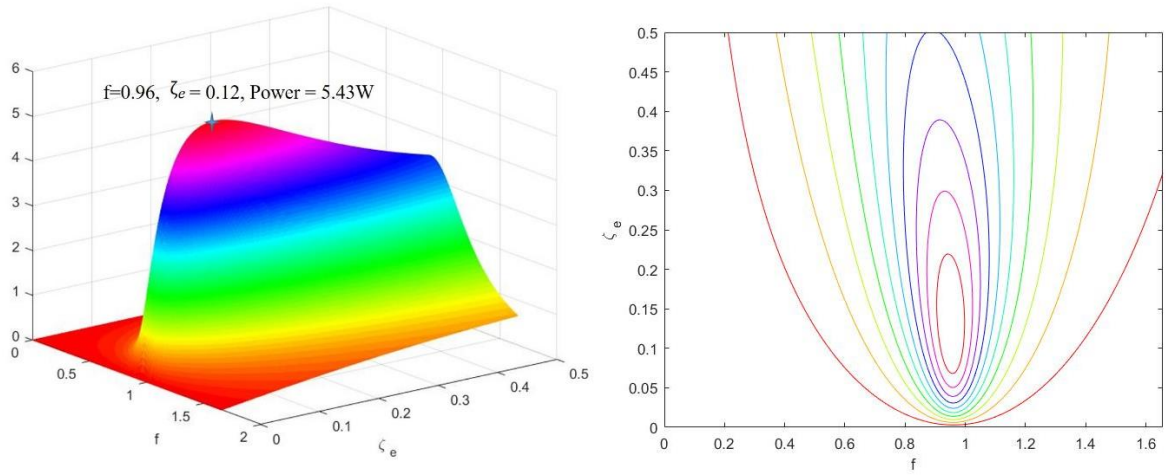

Figure 3-7 Traditional energy harvester result with dual mass model (a) average power at different tuning ratio and equivalent damping ratio ζ_e*, where the mechanical damping* ζ_m =10%. *(b) Contours of average power at different tuning ratio and equivalent damping ratio.*

3.5 MMR based energy harvester model

The MMR based energy harvester can be seen as a non MMR system with one added one disengaged period. Figure 3-6 shows the two periods of the MMR based energy harvester: engaged and disengaged period. Figure 3-7 (a) shows the comparison between input pinion speed and output shaft speed. It clearly shows the function of MMR system as a rectifier. In Figure 3-7 (b) shows the maximum average power of the MMR harvester model is 28.6W which is the highest power among three cases when $f = 0.6$ and $\zeta_e = 0.03$.

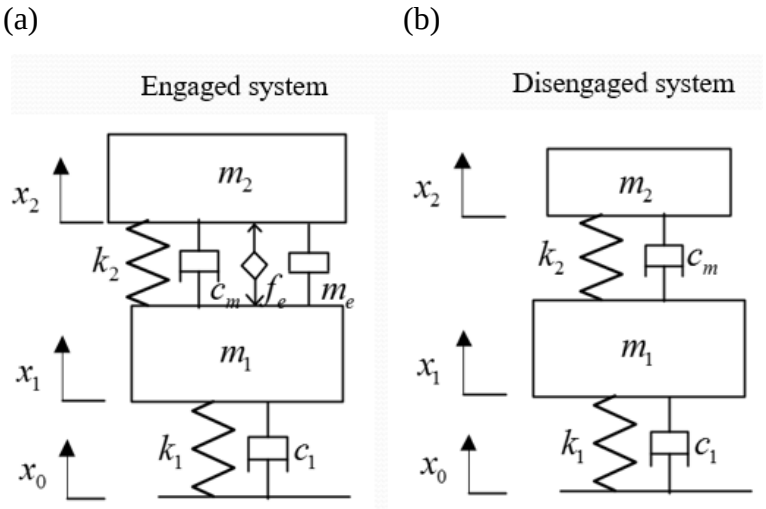

Figure 3-8 Two dof model of MMR based backpack energy harvester. (a) engaged system; (b)disengaged system.

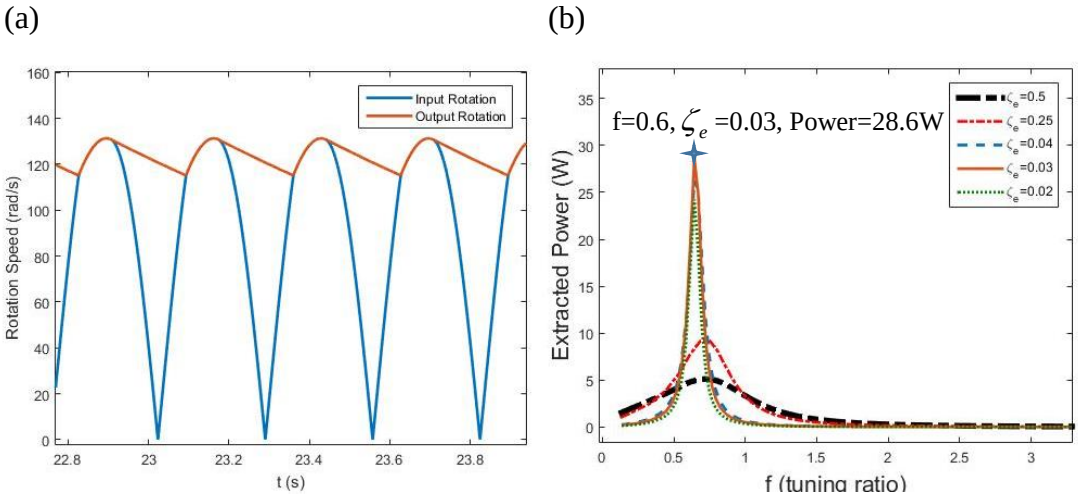

Figure 3-9 MMR based backpack energy harvester with dual mass model (a) Rotation speed of pinion and shaft when $k_2 = 2000\ N/m$ *under steady state. Engaged period and disengaged period. (b) Average power at different tuning ratio and electrical damping ratio* $\zeta_e = 0.02, 0.03, 0.04, 0.25$ *and* 0.5*, where the mechanical damping* $\zeta_m = 1\%$.

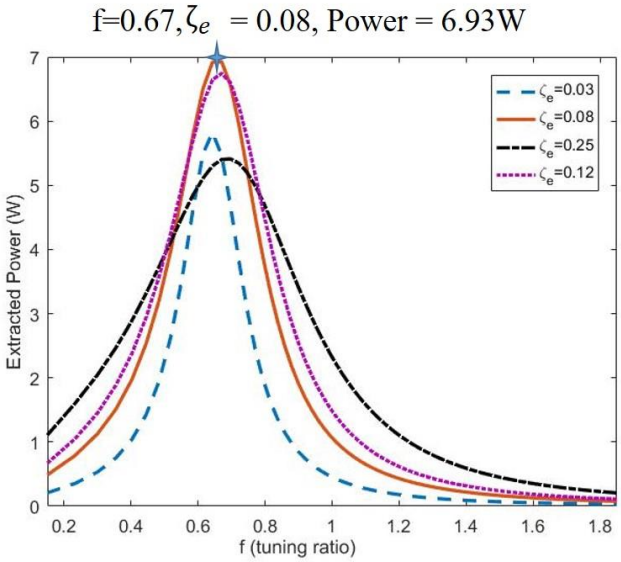

Figure 3-10 Average power at different tuning ratio and electrical damping ratio $\zeta_e = 0.03, 0.05, 0.08, 0.1$ *and* 0.25 *, where the mechanical damping* $\zeta_m = 10\%$ *in MMR based backpack energy harvester with dual mass model.*

For the three systems, pure viscous damping, non MMR, MMR, all achieve maximum power when at low ζ_e. However, the MMR harvester system can generate the largest average power among the three systems. The pure viscous damping system reached maximum power when tuning ratio is around 0.6, because the value of excitation frequency α ($\alpha = \frac{\omega}{\omega_1}$) is 0.6 and the optimal frequency is the same as the natural frequency of the base excitation. This is consistent with the conclusion of other researchers study about dual mass systems [35]. For the non MMR system, since we added one inertia in, which theoretically changes natural frequency ω_2, the optimal frequency is larger than the natural frequency of the base excitation.

Since MMR system equals to non MMR system with one added disengaged period, and the disengaged period is the pure viscous case without c_e in the system, the optimal power tuning ratio

value of MMR case at different ζ_e should between around the maximum power tuning ratio value of pure viscous case and that of non MMR case ($0.6 \le f \le 0.96$). Because the disengaged period duration time is related with c_e , and the smaller c_e is, the longer disengaged time period will be [36], when at low ζ_e , the maximum power of MMR system is around $f = 0.6$, like ζ_e =0.02 in Figure 3-9 (b), accordingly, when at relative high ζ_e , the maximum power is around $f = 0.9$, like ζ_e =0.5 in Figure 3-9 (b).

With the other two harvester models, pure damping model and traditional backpack energy harvester model as shown in Figure 3-4 and Figure 3-7, when the system mechanical damping ratio increase to 10%, the optimal power output are only 7.52W and 5.43W. The maximum power output occurs at same tuning ratio when system mechanical damping ratio is 1%, but at higher electrical damping ratio as system mechanical damping ratio increases. When the harvester system has 10% mechanical damping ratio, the maximum average MMR power output is 6.93W as shown in Figure 3-10.

3.6 Human comfort comparison simulation

3.6.1 Peak force

From [4] [5] and other researchers' work in the last few decades, there are few solid conclusions about elastically suspended backpack during human walking, like elastically-suspended load can reduce peak force and energy cost compared to rigid-attached backpack. In Chapter 3.6, peak force and human metabolic cost for three systems, pure damping, non MMR and MMR are discussed.

In this chapter, peak force are calculated from the total force acted on the human body mass m_1.

$$Peak\ Force = \max(m_1 \ddot{x}_1) \tag{3.12}$$

In this section, peak force of three systems we discussed before at different tuning ratio and electrical damping ratio has been shown in Figure 3-8, 3-9, 3-10.

(a) (b)

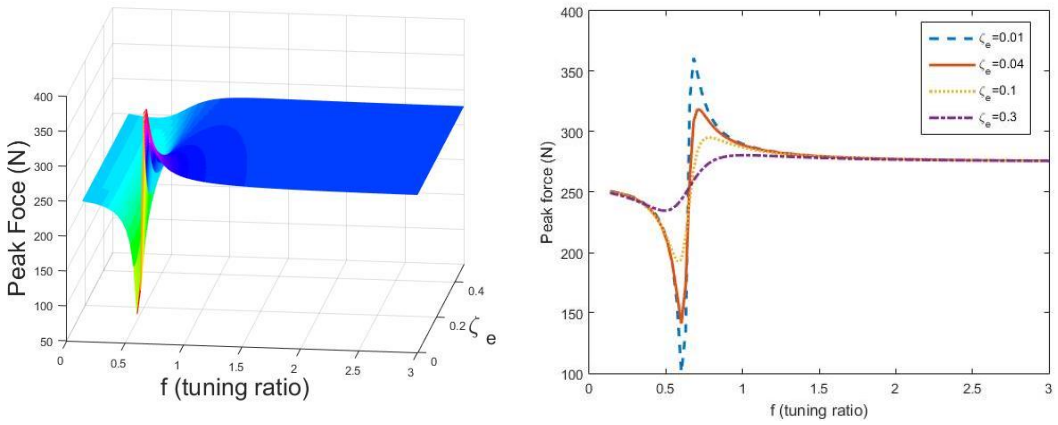

Figure 3-11 Peak force at different tuning ratio and electrical damping ratio ζ_e of pure damping system when $\zeta_m = 1\%$ (a) 3d contour plot; (b) 2d plot when ζ_e =0.01, 0.04, 0.1 and 0.3.

(a) (b)

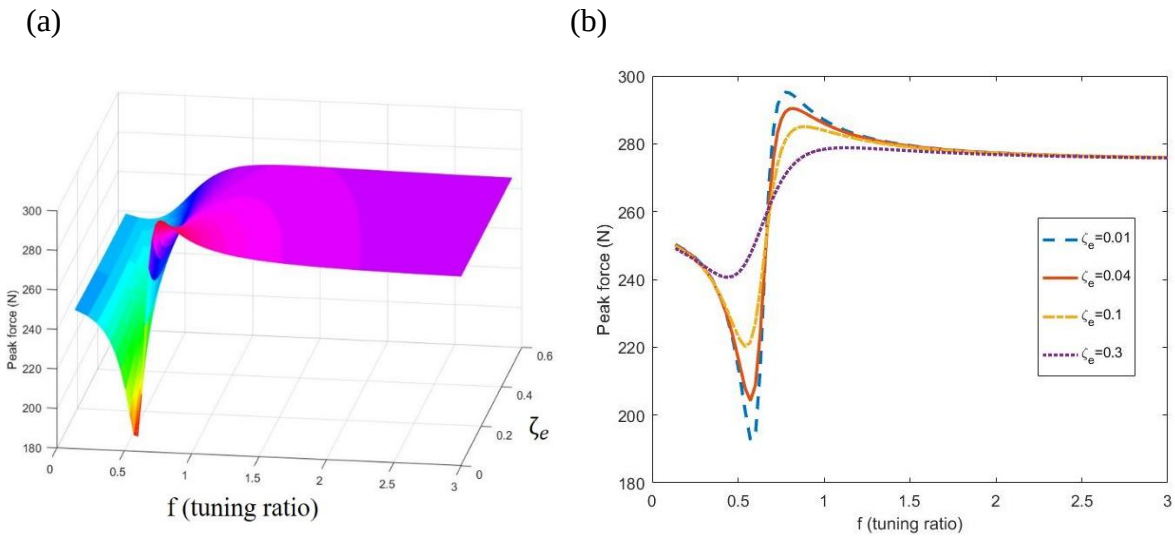

Figure 3-12 Peak force at different tuning ratio and electrical damping ratio ζ_e of pure damping system when $\zeta_m = 10\%$ (a) 3d contour plot; (b) 2d plot when ζ_e =0.01, 0.04, 0.1 and 0.3.

(a) (b)

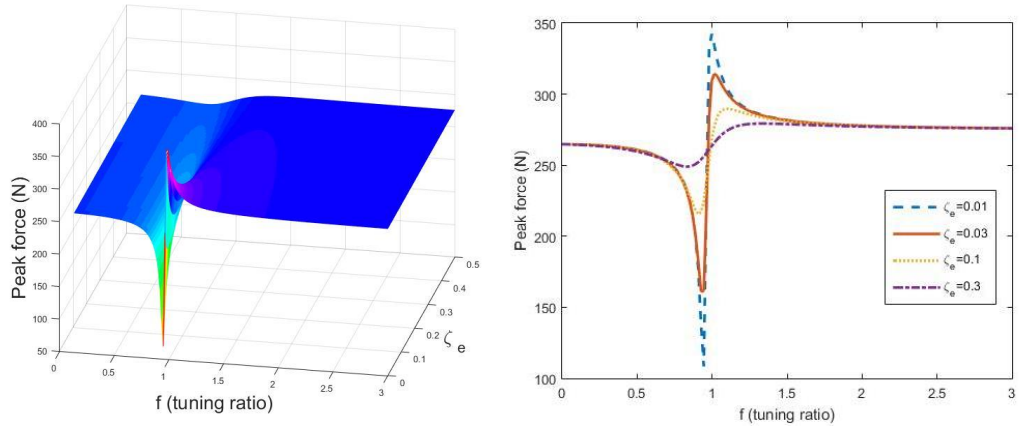

Figure 3-13 Peak force at different tuning ratio and electrical damping ratio ζ_e of non MMR system when $\zeta_m = 1\%$ (a) 3d contour plot; (b) 2d plot when ζ_e =0.01, 0.04, 0.1 and 0.3.

(a) (b)

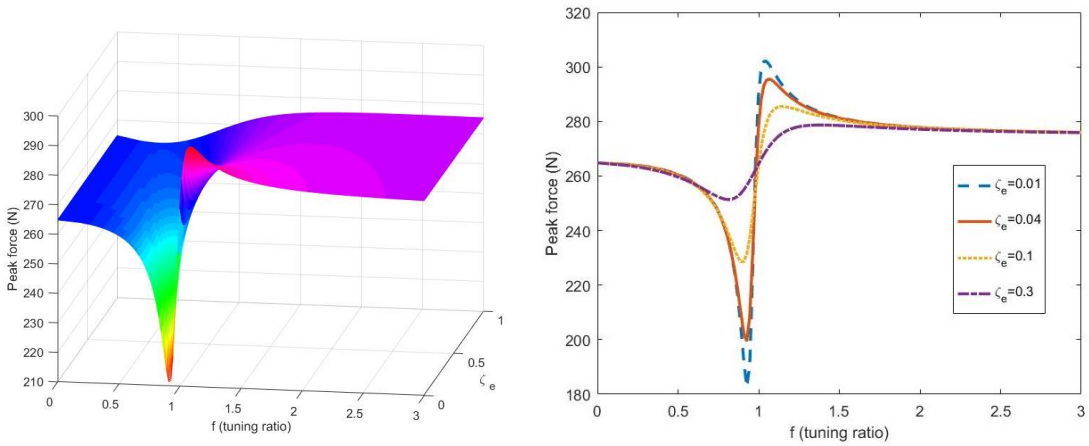

Figure 3-14 Peak force at different tuning ratio and electrical damping ratio ζ_e of non MMR system when $\zeta_m = 10\%$ (a) 3d contour plot; (b) 2d plot when ζ_e =0.01, 0.04, 0.1 and 0.3.

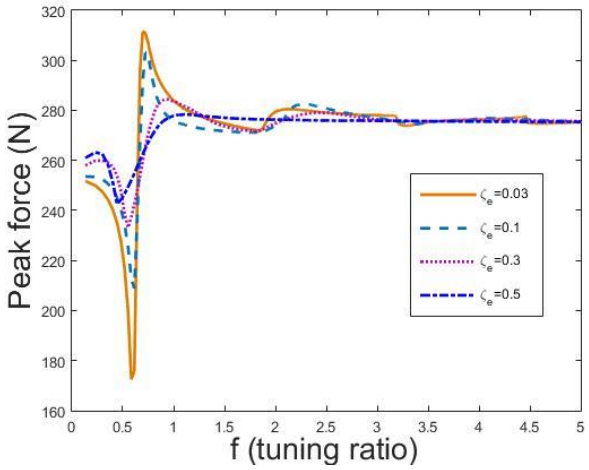

Figure 3-15 Peak force at different tuning ratio and electrical damping ratio ζ_e of MMR based harvester system when $\zeta_m = 1\%$.

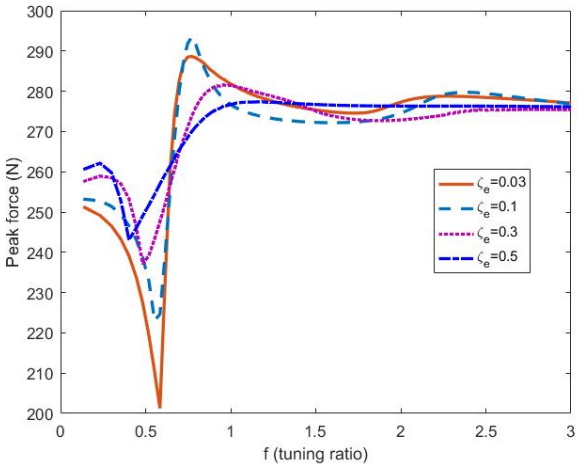

Figure 3-16 Peak force at different tuning ratio and electrical damping ratio ζ_e of MMR based harvester system when $\zeta_m = 10\%$.

When system mechanical damping ratio is 1%, the smaller the value of the peak force, theoretically the more comfortable the backpack will be for the human wearing the device. The smallest peak force value of pure damping case in Figure 3-11 is 91 N when $\zeta_e = 0$, and the smallest peak force value of non MMR system as shown in Figure 3-13 is 64 N when $\zeta_e = 0$. Since there's no close form solution for MMR case, the smallest ζ_e value we can simulate for peak force is 0.03, where the minimum peak force is 175N. Compared to the first two systems, non

MMR system has the smallest peak force value, but the minimum point appears at $\zeta_e = 0$, which in practical implementation means it doesn't harvest energy at all. However besides minimum point, in Figure 3-15, MMR has its advantage over non MMR case, when $0.98 < f < 2.2$, where the second peak of peak force for non MMR case in Figure 3-13, the peak force of MMR case is smaller than non MMR case. However, when the system mechanical damping ratio is 10%, the peak force as shown in Figure 3-12, 3-14 and 3-16, will show lower maximum peak force and higher minimum peak force compared with same case in 1% peak force value.

Both mechanical damping ratio study shows that MMR system has largest maximum peak force but smallest maximum value but has the largest minimum value among three types of harvesters.

3.6.2 Human energy efficiency

For energy harvesting from human body, the definition of good energy harvesting is not the larger energy it generated, the better the harvester it is any more. People have started to think about the tradeoff relationship between the power harvested and the human power consumed. To define the relation between the harvester power output and human metabolic cost, which we represent it using ground input power, we introduce a dimensionless quantity called 'human harvester efficiency', which is defined as:

$$\text{Human harvester efficiency} = \frac{\Delta \text{ metabolic power}}{\Delta \text{ electrical power}} \tag{3.13}$$

Where Δ means the difference between walking while harvesting energy and walking while rigid attached backpack. Which is similar to Cost of Harvesting in [4]. However, we compared with rigid attached backpack instead of walking while carrying the device but without harvesting energy.

Typically, the smaller the human harvester efficiency is, the better the energy harvester. This means you spend less metabolic cost but receive a larger electric output. For the human body of our dual mass system described above, we used ground input power as human metabolic cost.

$$Ground\ Input\ Power = [k_1(x_1 - x_0) + c_1(\dot{x}_1 - \dot{x}_0)]\dot{x}_0 \tag{3.14}$$

Figure 3-11 shows human harvester efficiency comparison in three systems at different tuning ratio when $\zeta_e = 0.2$. Overall, pure viscous damping case has the largest human harvester efficiency among the three systems. When $f \leq 0.8$, MMR has the smaller human harvester

efficiency value than non MMR case, and is the better to use for backpack energy harvesting from the human body.

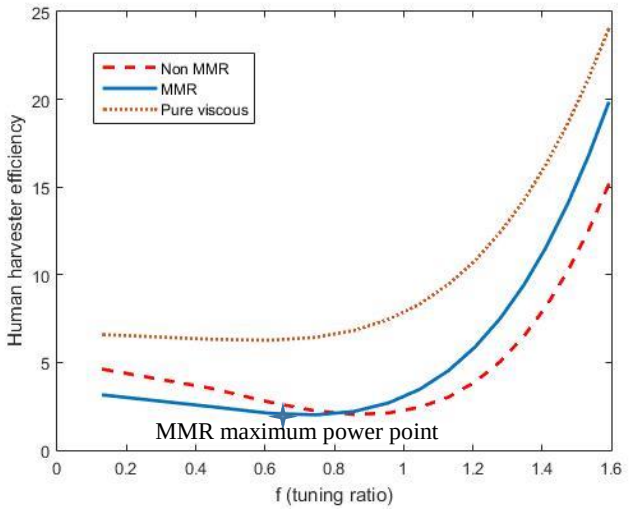

Figure 3-17 Human harvester efficiency comparison of three systems, pure viscous system, non MMR system and MMR system at different tuning ratio when $\zeta_e = 0.2$.

3.7 Discussion about dual mass model

Human walking is a very comprehensive activity. In most literatures, researchers who studied suspended load backpack are focused on experiment like [13]. However, with a model which could describe human walking, it could help us better simulate with different spring stiff, different types of harvester, or different load instead of letting people repeat the experiment again and again. In this chapter, we have simulated human COM motion during walking as a simple dual mass system under base excitation. In this case, simulation results could be calculated easily, like the maximum power output, human input and comparison in three types of harvester without considering stability of different parameters, different human parameters could be applied in the system, etc.. This dual mass model is our first trial on human walking model with suspended load backpack harvester. However, with the dual mass model we have showed, we cannot simulate results other researchers' experiments, vertical COM different amplitude at upward motion and downward motion, M-shaped vertical GRF, like shown in Figure 3-11.

(a) (b)

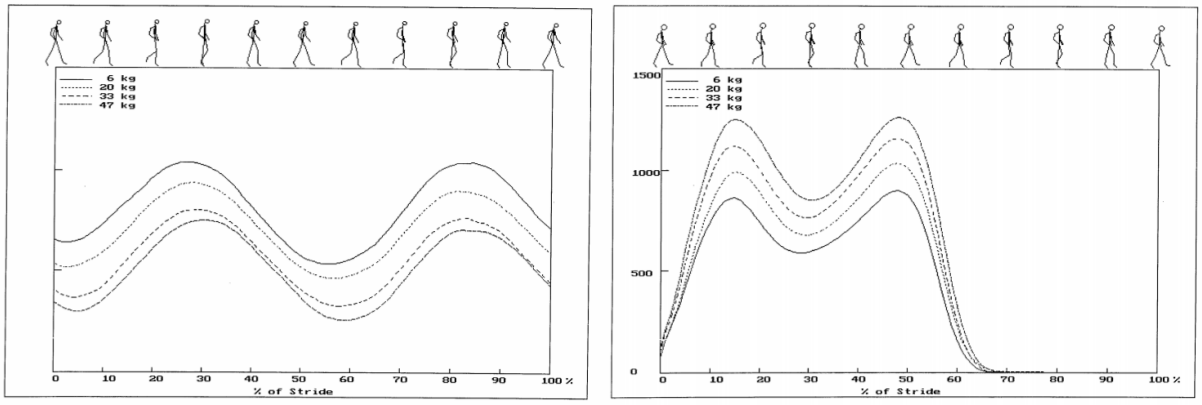

Figure 3-12 Experiment data of load effect [13]: (a) for vertical COM motion (cm); (b) for vertical GRF (N).

3.8 Chapter summary

In this chapter, three dual mass vibration models have been proposed for different types of harvesters: pure viscous damping vibration, traditional (non MMR) energy harvester and MMR based energy harvester. MMR based energy harvester has an absolute advantage over the other two types in the power output at low electrical damping ratio ζ_e with up to 28.6W average power. We also take the human comfort factor into consideration. By comparing human peak force of these three types of harvesters, non MMR harvester has the smallest minimum value, but in certain range of tuning ratio ($0.98 < f < 2.2$), the MMR based harvester is more comfortable to human body. To better understand the tradeoff relationship between human comfort and harvester power output, we introduced a new term called 'Human harvester efficiency'. In the human harvester efficiency comparison, overall, pure viscous system costs more additional human metabolic cost than the other two systems when generate the same amount of electrical power output when $\zeta_e = 0.2$. When $f \leq 0.8$, MMR system has the smallest human harvester efficiency value.

4. A bipedal walking with suspended load model

4.1 Chapter Introduction

In this chapter, a bipedal walking with suspended load model, a bipedal walking model, is introduced for better mimicking behaviors of human walking than simple dual mass model. The stability, optimal parameters for power output and limitations and future work will also be discussed. Jeffrey Ackerman and Justin Seipel and some other researchers [37] [38] studied the effect of suspended-load backpack on human body by using a simple dual mass system in which a stable locomotion can be easily achieved by sinusoidal force or displacement input from ground or spring leg. However, human walking appears to be much more complicated than that in [37] [38], a bipedal walking modeling could better illustrates human walking pattern, such as vertical COM motion, and Ground Reaction Force (GRF). There are mainly two types of bipedal dynamics modeling of walking and running, the inverted pendulum model and the spring-mass model [22] [39] [40] [41] [42]. Geyer et al. has shown that a simple bipedal spring-mass model can essentially explain the basic walking mechanics and the model-predicted stance dynamics of spring-mass system can better fit that of experimental data than the inverted pendulum system in vertical displacement, horizontal and vertical Ground Reaction Forces (GRFs) [39]. For instance, the inverted pendulum model could not reproduce the M-shaped vertical GRF during walking, but spring-mass walking model could. Based on spring-mass walking model, we have developed our bipedal human walking with suspended load backpack model. It is the first model that integrated human walking with suspended load.

4.2 Bipedal dynamics human walking model

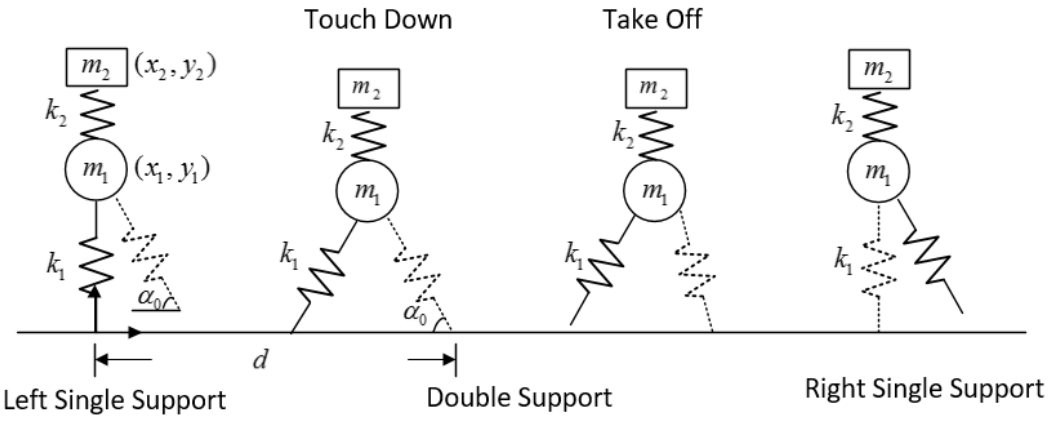

Figure 4-1 The spring-mass walking with suspended backpack model.

The spring-mass walking with suspended load backpack model as shown in Figure 5 represents human body mass m_1 at the COM and its motion is described as (x_1, y_1) of the body and backpack as m_2 and its motion is defined as (x_2, y_2). The two legs are modeled as two independently massless, linear springs with rest length of l_0 and stiffness of k_1. Meanwhile, suspended load backpack is connected with human body m_1 by one massless, linear spring with its stiffness of k_2, which is always perpendicular to the ground. We assumed that at each step, the touchdown angle α_0 remains the same. The other assumption we made is that there is no energy loss during transition between swing and stance phase.

A complete step starts from one point in left single support when the left spring leg (solid line spring in Figure 4-1) is vertical to the ground and ends when the right spring leg (dashed line spring in Figure 4-1) is vertical to the ground. The step distance d denotes the distance between each step. Since we assumed that the suspended load backpack is always perpendicular to the ground, $x_1 = x_2$.

The equation of motion at left single support in step i (i=1, 2, 3…) is:

$$\begin{cases} (m_1 + m_2)\ddot{x}_1 = Px_1 \\ m_1\ddot{y}_1 = Py_1 - m_1 g + k_2(y_2 - y_1) \\ m_2\ddot{y}_2 = -m_2 g - k_2(y_2 - y_1) \end{cases} \tag{4.1}$$

Where $P = k_1(\frac{l_0}{\sqrt{x_1^2 + y_1^2}} - 1)$. The left single support ends and double support phase starts when $y_0 = l_0 \sin\alpha_0$. The equation of motion at double support phase in step i is:

$$\begin{cases} (m_1 + m_2)\ddot{x}_1 = Px_1 - Q(d - x_1) \\ m_1\ddot{y}_1 = Py_1 + Qy_1 - m_1 g + k_2(y_2 - y_1) \\ m_2\ddot{y}_2 = -m_2 g - k_2(y_2 - y_1) \end{cases} \tag{4.2}$$

Where $Q = k_1(\frac{l_0}{\sqrt{(d - x_1)^2 + y_1^2}} - 1)$. The double support phase finishes when the left spring leg take off from the ground where $\sqrt{(d - x_1)^2 + y_1^2} = l_0$ and that's when right single support phase begins. The equation of motion at right single support phase in i-th step:

$$\begin{cases} (m_1 + m_2)\ddot{x}_1 = -Q(d - x_1) \\ m_1\ddot{y}_1 = Qy_1 - m_1 g + k_2(y_2 - y_1) \\ m_2\ddot{y}_2 = -m_2 g - k_2(y_2 - y_1) \end{cases} \tag{4.3}$$

The full step is completed when $\dot{y}_1 = 0$, which is vertical velocity of m_1 is zero.

The parameters we used to study this model are listed in Table 4-1.

Table 4-1 Parameters values for model of walking with suspended load backpack

Human body mass	m_1	80kg
Suspend load mass	m_2	15kg
Human leg spring stiffness	k_1	14000N/m [37] [34] [42]
Suspended backpack spring stiffness	k_2	2000N/m
Spring leg rest length	l_0	1m

Compared with simple one dof system which is shown in Figure 4-2, our bipedal walking model with suspended load backpack is much more realistic to real world human walking situation. The parameters we have used to simulate one dof model same m_2, k_2 as list in Table 4-1. Mechanical friction may be caused by linear guide of suspended load backpack, which we represent by c_2 =

50 N-s/m. The model has one frequency sinusoid inputy_1, and $y_1 = 0.025 * \sin(10.47t)$ [37], which we assumed that human walking at 3.36mph (1.5m/s) with 5cm peak to peak COM motion. The right figure in Figure 4-2 shows human COM motion and vertical GRF results of 1 dof model, which is just simple sinusoid wave.

However, human walking vertical GRF results is much more complicated than just sinusoid wave. For example, during human walking, vertical GRF should be in an M shape like in Figure 4-3. Human vertical COM motion contains multiple frequency as shown in Figure 4-3 which is totally different than simple sinusoid wave input human vertical COM motion result.

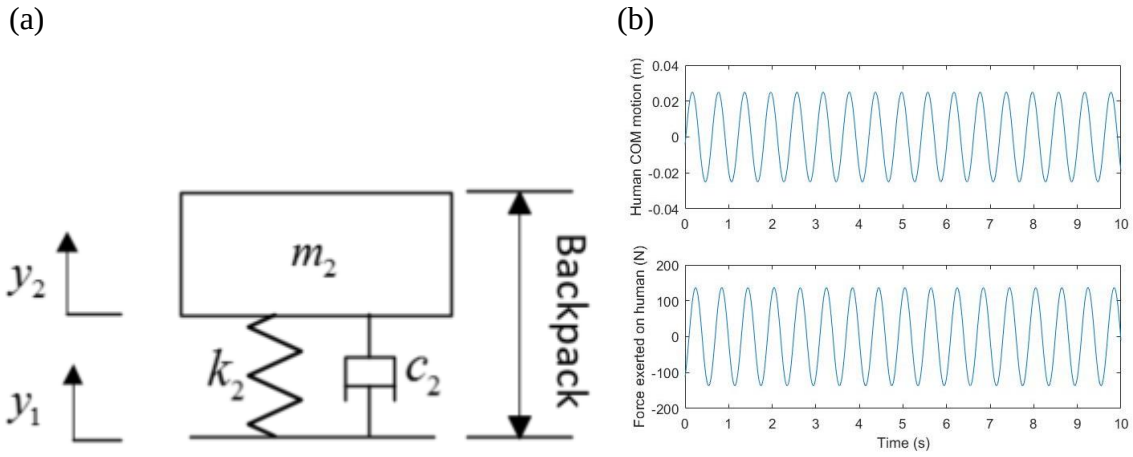

Figure 4-2 One dof model with sinusoidal input (a) COM result; (b) vertical GRF results.

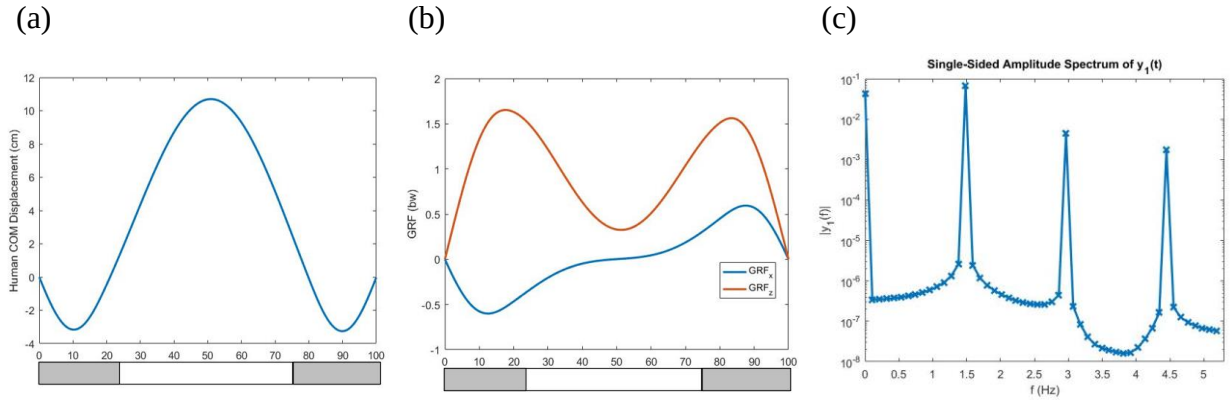

Figure 4-3 Results of bipedal walking with 15kg suspended load model under condition of α_0 *=61 ° with initial walking speed is 1m/s and backpack system energy is 160J. (a) vertical COM result; (b) vertical GRF result. Gray area is double support phase while white area represents single support phase. (c) frequency content of vertical COM motion showed in (a).*

4.3 Stability

Stability is an important aspect for bipedal walking model. Since this spring mass walking system is a conservative system, there are two more parameters need to be determined to completely describe the motion of the model, angle of attack α_0 and backpack system total energy E_2. Since the body m_1 has no vertical velocity which means that $\dot{y}_1 = 0$, the backpack system total energy E_2 is directly related to y_2 when we set the initial walking speed x_1 and $\dot{y}_2$. The stable state solutions for this model is calculated by a Newton-Raphson algorithm [42] by using ode45 in MATLAB. In each step, we set an initial height of spring leg y_{10}, angle of attack α_0 and backpack system energy E_2 to see whether we have a fixed point in the return map. The study shows that walking speed and angle attack have significant influence on fixed points results as shown in Figure 4-5 in which we have drawn solutions in different backpack system energy E_2 at initial walking velocity of 1m/s and 1.1m/s. We could also observe that the smaller walking velocity is, the wider range of fixed points with respect to angle of attack and initial height of spring leg.

Angle of attack will affect symmetry and peak value of human walking gait pattern as shown in Figure 4-5 as systematically described by [42] using spring – mass walking model. Set E_2=160J $(v_1)_0 = 1m/s$ as an example. Vertical COM displacement of α_0 =61° , which we describe it as point A as is shown in Figure 4-4, is larger than that of point B when α_0 =67° . With α_0 =67°, the first peak value of vertical GRF is larger than it in α_0 =61° while the second peak value of vertical GRF is smaller than that in α_0 =61° which has a similar trend with conclusion in [39].

We also check the frequency content of different vertical COM pattern with different walking parameters, angle of attack, backpack energy level, and initial walking velocity, as shown in Figure 4-6. As we can see, angle of attack has the largest impact to frequency shift and the value of the dominant frequency. However, the initial walking velocity will not impact too much about frequency content at low frequency, but only constant value, which is the value at the zero frequency. The backpack energy level will not influence dominant frequency value and the constant but only high frequency.

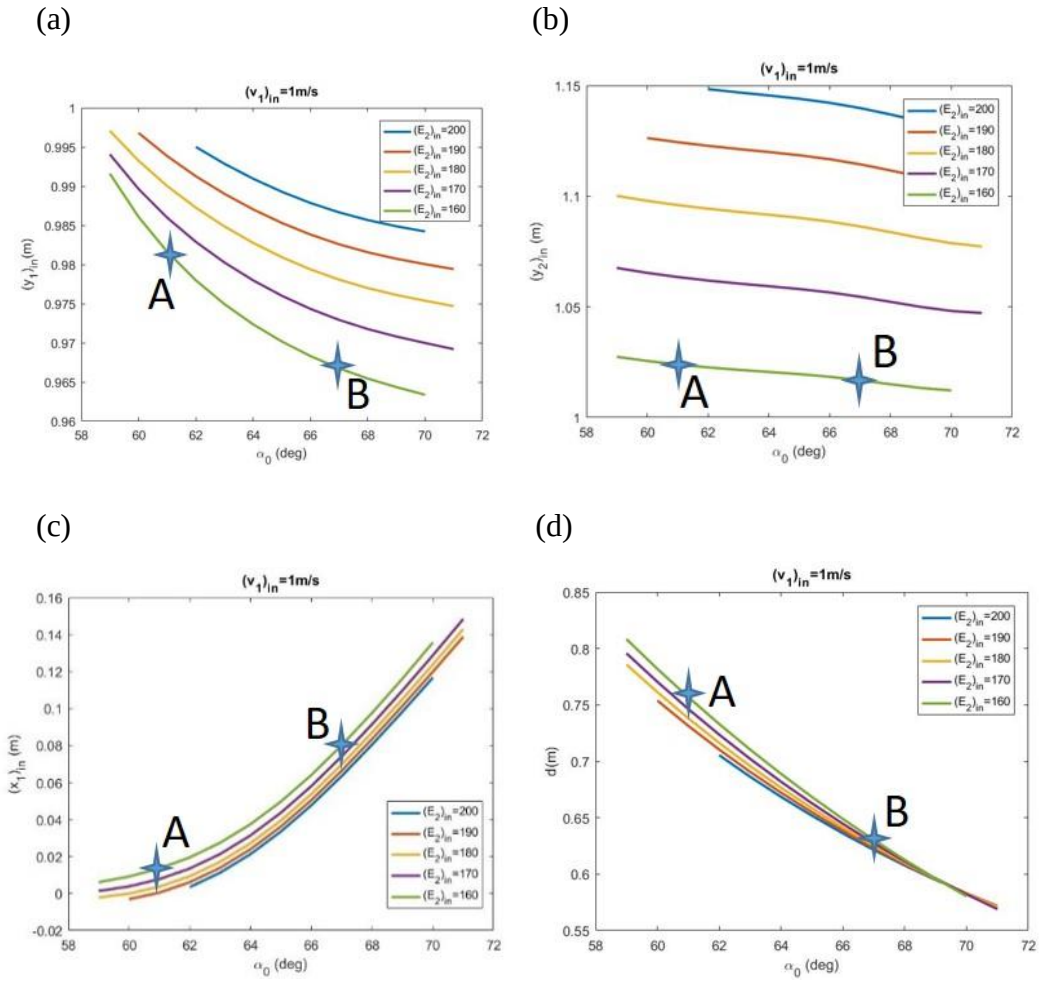

Figure 4-4 Fixed points solutions at different initial backpack energy E_2 level when initial walking speed $(v_1)_{in}$ =1m/s.(a) angle of attack α_0 with respect to initial height of spring leg $(y_1)_{in}$,(b) angle of attack α_0 with respect to initial height of backpack position $(y_2)_{in}$ (3) angle of attack α_0 with respect to initial horizontal position of human body $(x_1)_{in}$ (d) angle of attack α_0 with respect to step distance d .

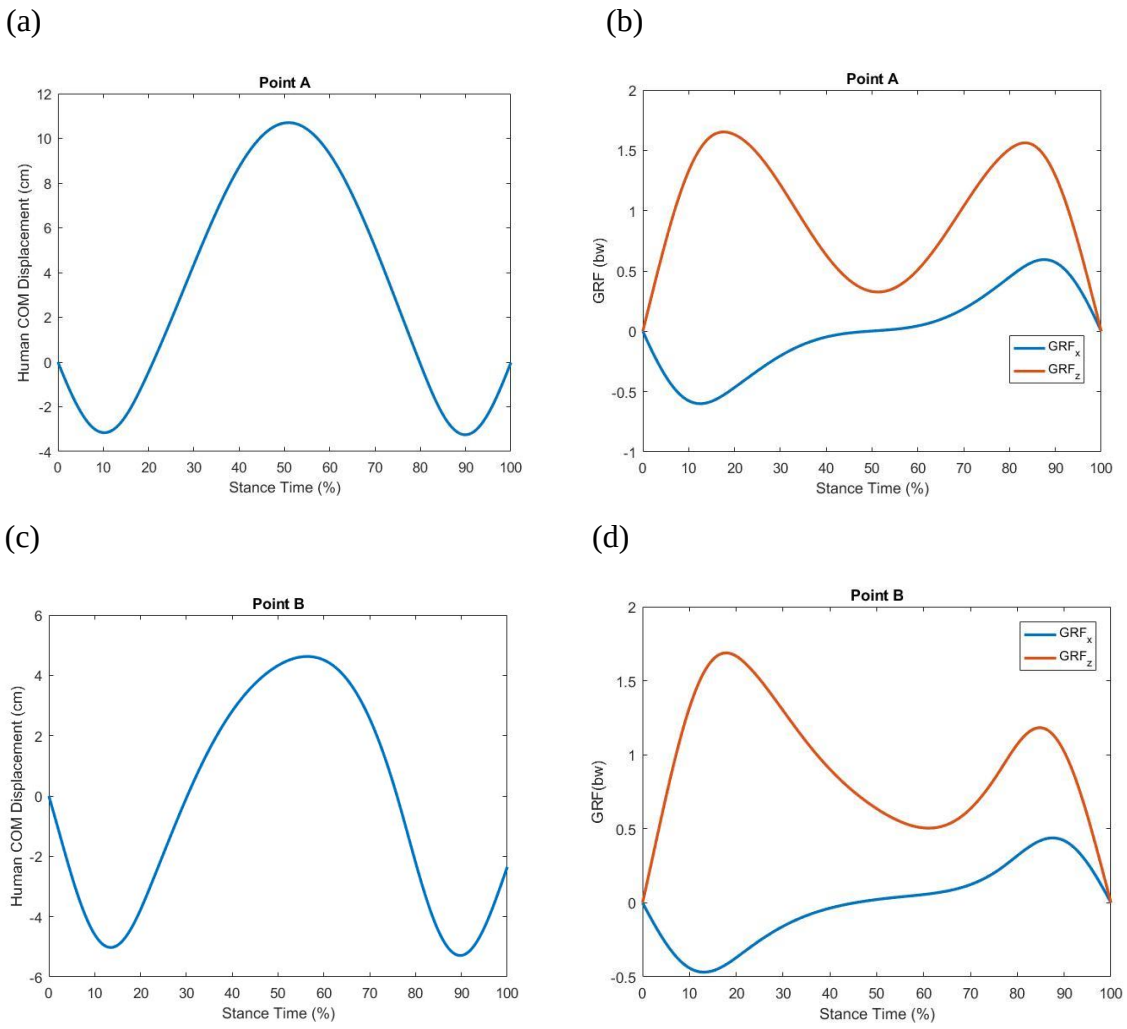

Figure 4-5 GRF and vertical COM motion at point shown in Figure 4-4. Point A and Point B are 61° and 67° at $(E_2)_{in}$=160J with $(v_1)_{in} = 1m/s$. (a) vertical COM motion result of point A; (b) vertical GRF result of point A; (c) vertical COM motion result of point B; (d) vertical GRF result of point B.

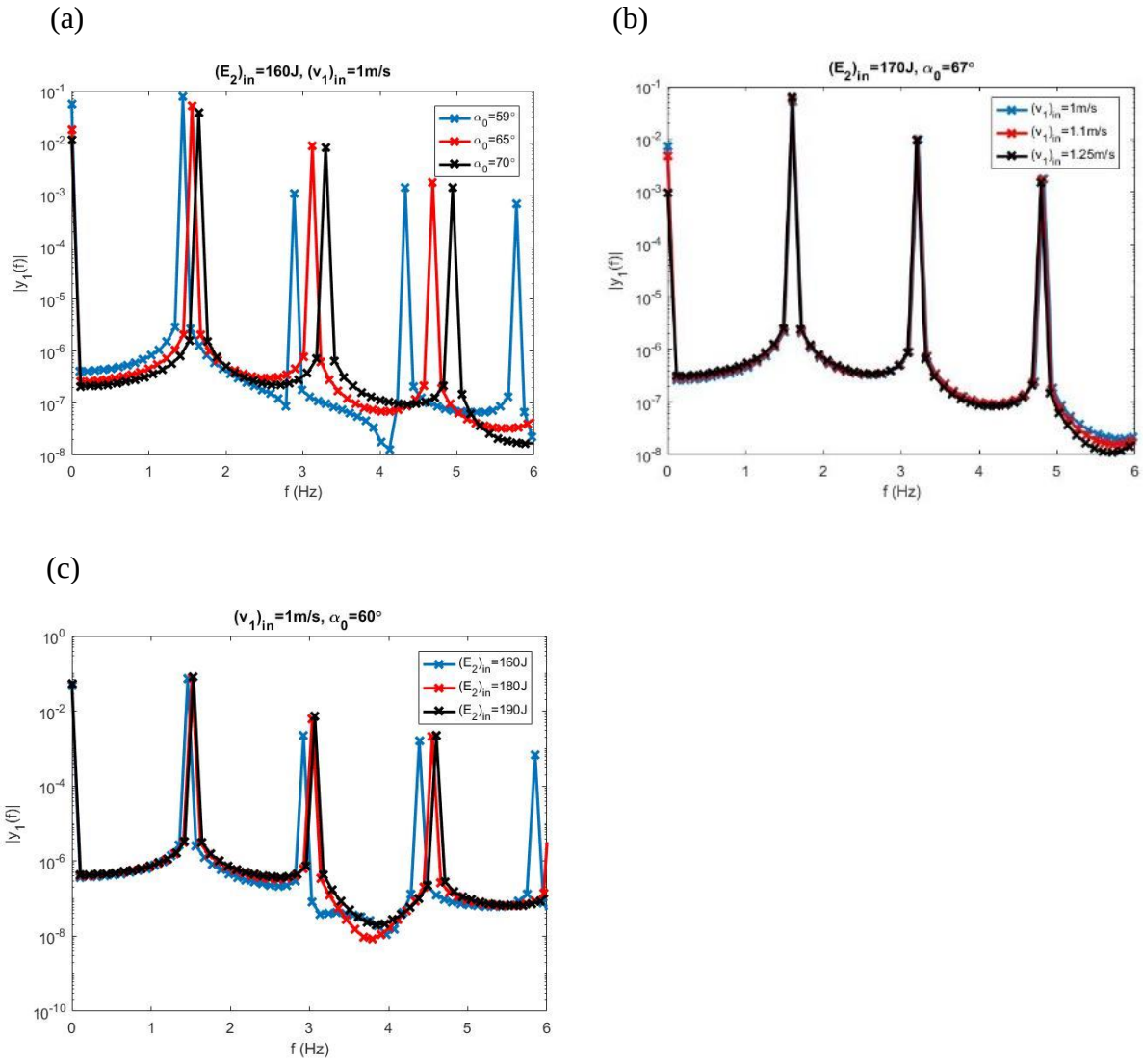

Figure 4-6 Frequency content of COM motion in different condition. (a) vertical COM motion result in frequency domain at different angle of attack when $(E_2)_{in} = 160J$ *and* $(v_1)_{in} = 1m/s$*; (b) vertical COM motion result in frequency domain at different initial walking velocity* $(E_2)_{in} = 170J$ *and* $\alpha_0 = 67°$*; (c) vertical COM motion result in frequency domain at backpack energy level* $(v_1)_{in} = 1m/s$ *and* $\alpha_0 = 60°$.

4.4 Comparison in MMR based and traditional backpack energy harvester

The main purpose of developing bipedal walking model with suspended load backpack model is to generate realistic human vertical COM motion which contains multiple frequency. Thus, we

could then compare traditional backpack energy harvester and our MMR based backpack energy harvester. We assumed that even though we add the harvester between m_1 and m_2, human walking gait with COM movement will not be significant influenced and human would adopt themselves to different walking situation. Hence, we used vertical COM displacement we got from bipedal walking with suspended load walking model as an input and simulate our MMR based backpack energy harvester and tradition backpack energy harvester output used models in Figure 4-7.

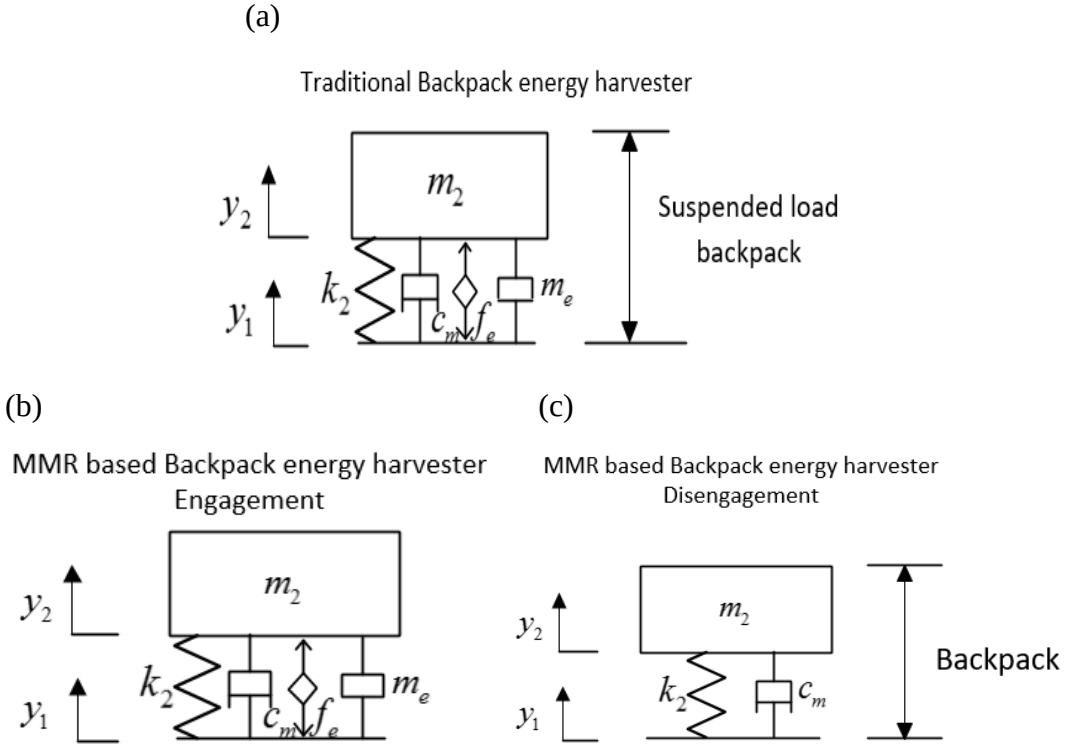

Figure 4-7 One dof model (a) traditional backpack energy harvester model. (b) MMR based backpack energy harvester engagement (c) MMR based energy harvester disengagement model.

Figure 4-8 and 4-9 shows voltage output of the Point A and Point B showed in Figure 4-4 when energy harvester system has 5% mechanical damping ratio case and 10% mechanical damping ratio case. It clearly showed different peak value of upward motion and downward motion. Compared with 5% and 10% mechanical damping ratio cases, larger mechanical damping ratio in the system has smaller power output peak value. Accordingly, power output of larger mechanical damping ratio has smaller average power output. Figure 4-10 shows comparison of the average output power in non MMR and MMR based backpack energy harvester with respect to $(y_1)_0$ and angle of attack α_0. We can see that, in general, the larger walking velocity is, the higher electrical

power output will be. In addition, MMR based backpack energy harvester could generate larger output power than traditional backpack energy harvester.

To better understand the reasons why MMR based backpack energy harvester has much better output performance than traditional energy harvester under all human walking conditions considered, we studied its amplitude spectrum as shown in Figure 4-11. We compared the maximum and minimum power output different point of MMR and traditional backpack energy harvester when $(v_1)_0 = 1m/s$. We can see that no matter how minimum difference in power output, it won't even close to one frequency sinusoid input. In addition to it, the higher frequency content of vertical human COM motion has, the larger power output difference it will be and the better MMR based backpack energy harvester power output will be compared with traditional backpack energy harvester.

(a)

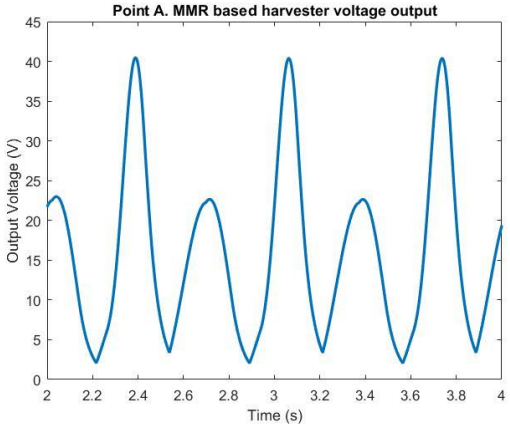

(b)

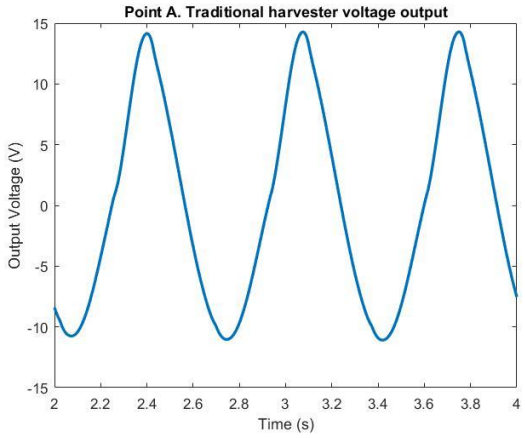

(c)

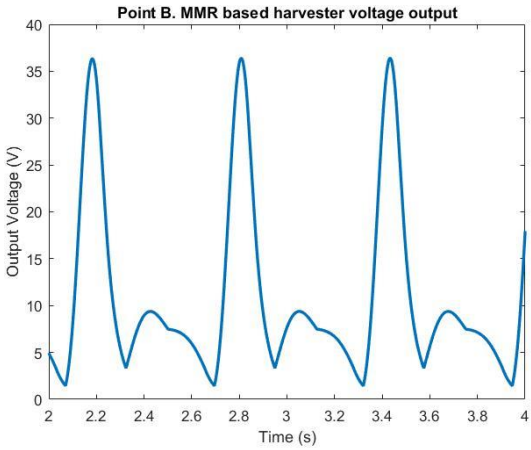

(d)

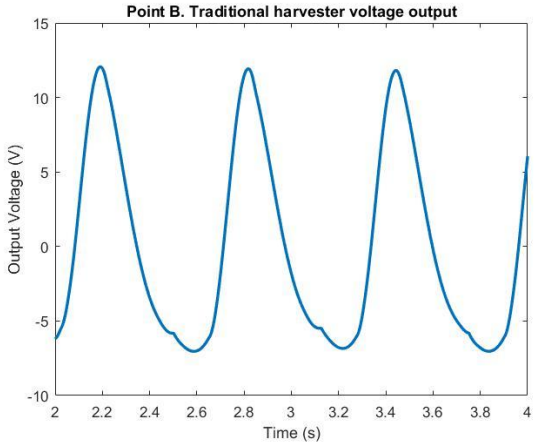

Figure 4-8 (a) output voltage of MMR based backpack energy harvester at point A with 5Ω external resistor; (b) output voltage of traditional backpack energy harvester at point A with 5Ω external resistor; (c) output voltage of MMR based backpack energy harvester at point B with 5Ω external resistor; (d) output voltage of traditional backpack energy harvester at point B with 5Ω external resistor; Point A and Point B have been shown in Figure 4-4 when system mechanical damping ratio ζ_m *is 5% and external resistor is 5Ω .*

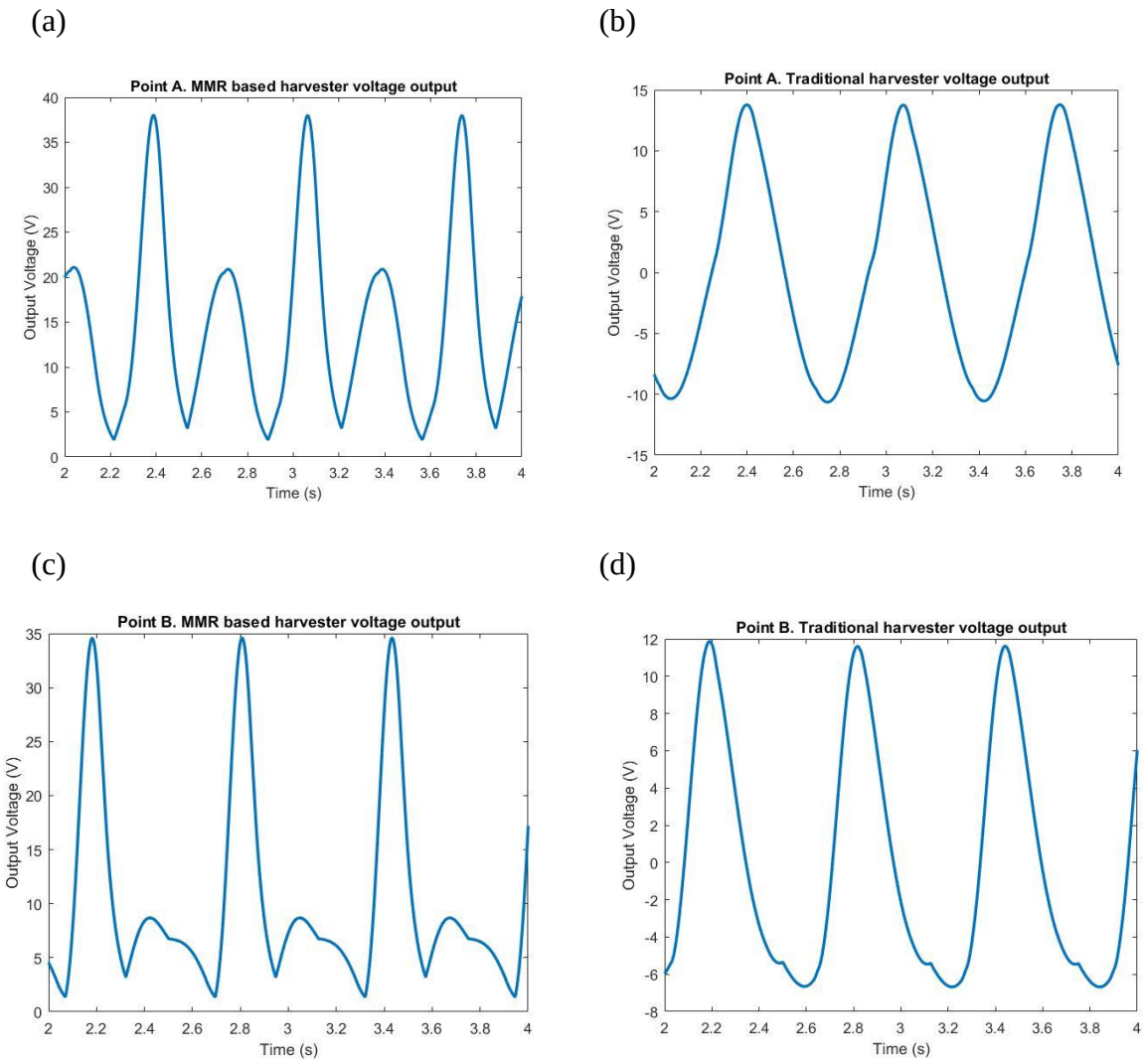

Figure 4-9 (a) output voltage of MMR based backpack energy harvester at point A with 5Ω external resistor; (b) output voltage of traditional backpack energy harvester at point A with 5Ω external resistor; (c) output voltage of MMR based backpack energy harvester at point B with 5Ω external resistor; (d) output voltage of traditional backpack energy harvester at point B with 5Ω external resistor; Point A and Point B have been shown in Figure 4-4 when system mechanical damping ratio ζ_m *is 10% and external resistor is 5Ω .*

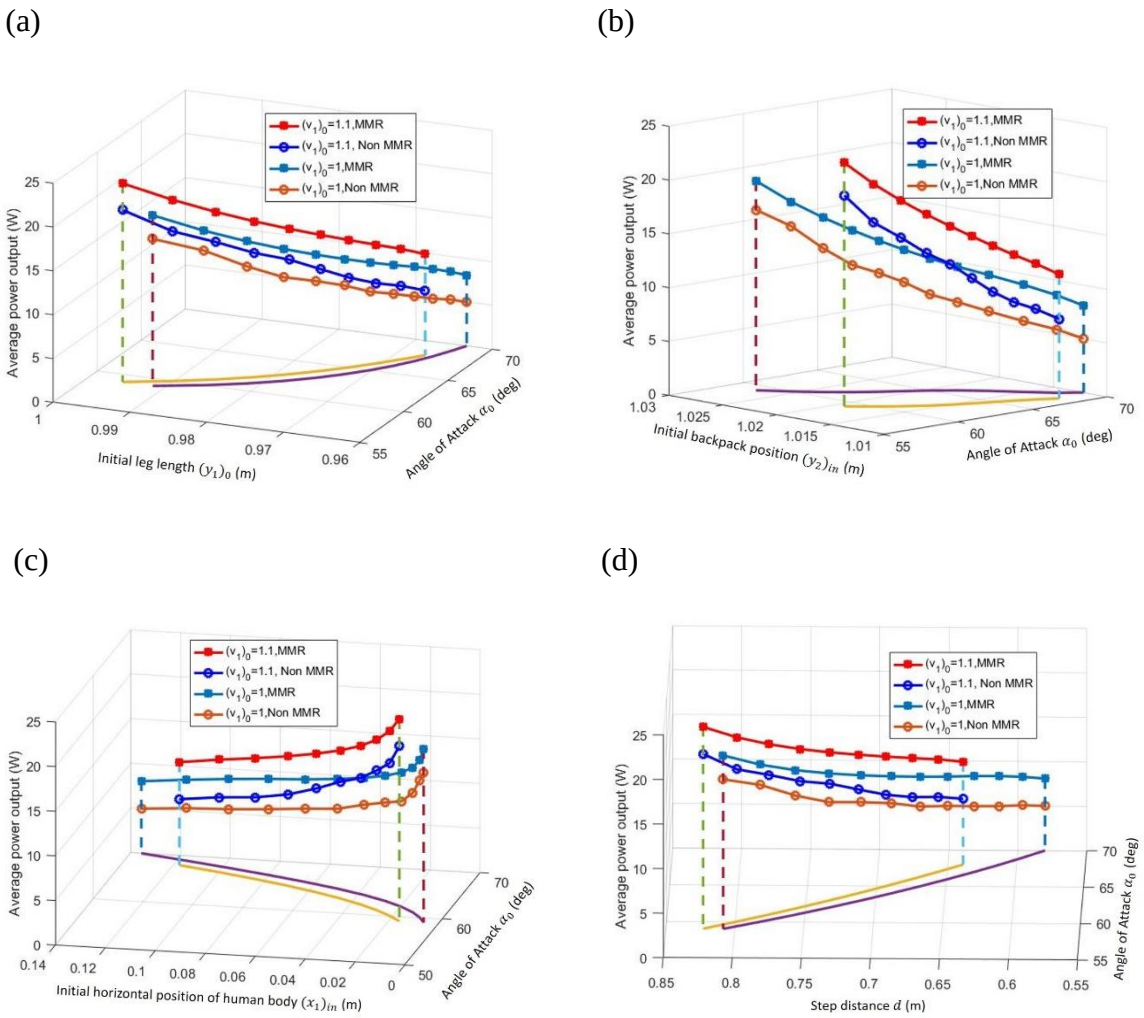

Figure 4-10 Average electrical power simulation results of two types of harvester, traditional backpack energy harvester and MMR based backpack energy harvester when $(E_2)_{in}$ *=160J and mechanical damping ratio is 5%: (a) angle of attack with respect to initial height of spring leg at different initial speed; (b) angle of attack with respect to initial backpack position at different initial speed; (c) angle of attack with respect to initial human body horizontal position at different initial speed; (d) angle of attack with respect to step length at different initial speed.*

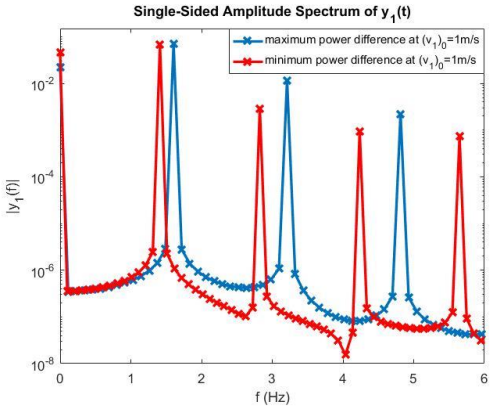

Figure 4-11 Single-sided amplitude spectrum in frequency domain comparison in maximum power difference point and minimum power difference point at all conditions consider at $(v_1)_0 = 1m/s$.

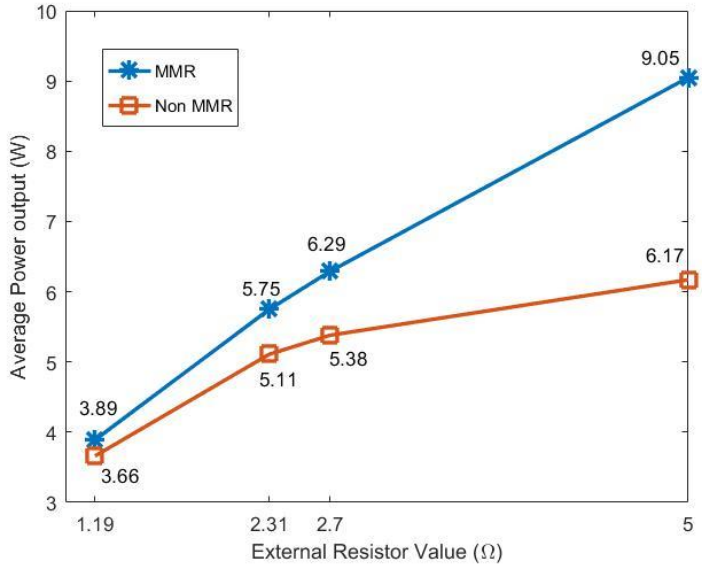

Figure 4-12 Average power output with respect to different external resistor values in two types of harvester, MMR based backpack energy harvester and Non MMR (traditional) backpack energy harvester when system mechanical damping ratio is 10% and human walking gait input is Point B shown in Figure 4-4.

In Figure 4-12, we have discussed average power output with respect different external resistor values, 1.19 Ω, 2.31 Ω, 2.7 Ω and 5Ω which the same as human treadmill test in Chapter 5. As we can see in Figure 4-12, MMR based energy harvester always has larger power output than traditional energy harvester. In addition, the optimal resistor value for traditional backpack energy

harvester power output is 2.7 Ω. However, for MMR based energy harvester power output is in an increasing trend as resistor increase before 5 Ω, which human treadmill tests shows similar trend.

4.5 Improved bipedal walking model

For energy harvesting, the bipedal walking model we have introduced previously in this chapter could also be improved into a model with harvester between human body mass and backpack mass, which means directly combine the harvester and walking model.

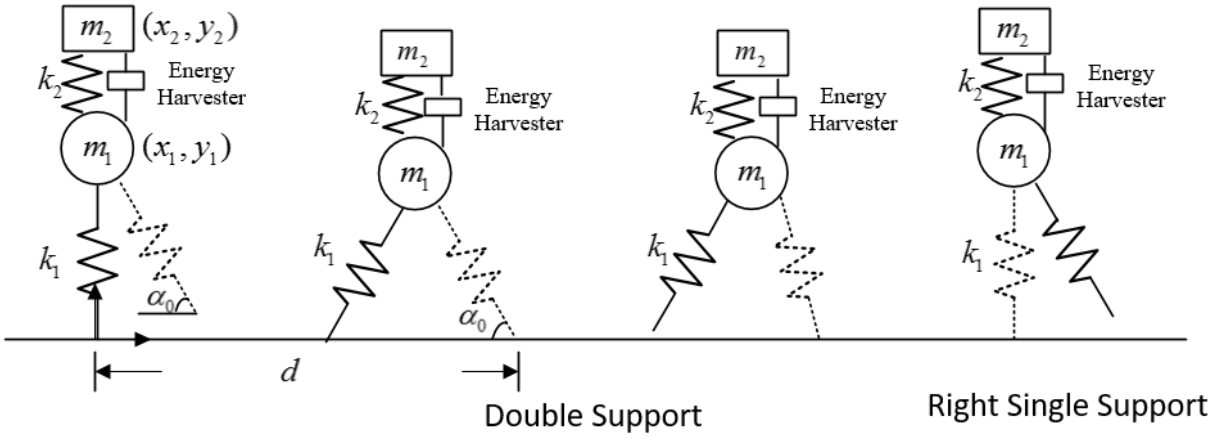

Figure 4-13 The spring-mass walking with suspended backpack energy harvester model (improved bipedal model).

In this model, we put constant walking velocity (horizontal velocity of m_1) as an additional input for the model. Thus, the model could continuous walking with harvester extracting power out at the same time. For this model, we currently have looked into improved bipedal walking model with traditional energy harvester.

Figure 4-14 has shown simulation result of power output with respect to different resistors with traditional backpack energy harvester with two walking speed, 2.5 mph and 3mph. Since the model has completely changed, some parameters of human body has changed. Human leg spring stiffness, k_1 = 38000 N/m, and angle of attack here is α_0 = 76°. The maximum power when walking with 2.5 mph is 1.35W when external resistor is 1.1 Ω. In addition, the maximum power when walking with 3 mph is 10.4 W when external resistor is 0.65 Ω.

However, this bipedal walking model with MMR based energy harvester much more complicated to simulate than traditional energy harvester, which will be considered in the future by other teammates in the team.

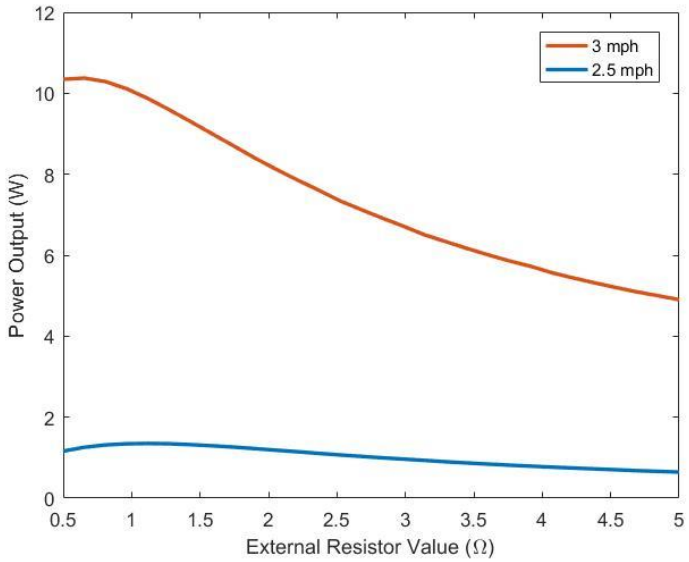

Figure 4-14 Average power output with respect to different external resistor values while wearing traditional backpack energy harvester in two walking speed, 2.5mph and 3mph, when initial leg length is 1m, 10% mechanical damping ratio of the harvester system, $\alpha_0 = 76°$, m_1 *=80kg,* m_2 *=15kg,* k_1 *=38000 N/m,* k_2 *=2000 N/m and the harvester parameters are the same as previously mentioned.*

4.6 Chapter summary

In this chapter, we studied MMR based backpack energy harvester and traditional energy harvester under complicated multiple frequency input as human vertical COM motion. We developed a novel bipedal spring-mass human walking with suspended load model to simulated complicated human COM motion. This bipedal spring-mass bipedal walking with suspended load model is the first initial trial to integrate complicated human walking gait into energy harvester modeling. This model still has some drawbacks like overestimating vertical COM motion. To better describe human walking with backpack energy harvester, an improved bipedal walking model has also been developed. However, there is still room we could do to improve this model in

the future study. Overall, MMR system has larger power output and higher mechanical efficiency and reliability compared with traditional rack pinion system under multiple frequency input as human walking.

5. Human experiment

5.1 Chapter Introduction

In this chapter, we conducted experiment to verify the advantages of our MMR base backpack energy harvester we mentioned in previous several chapters, larger power output, higher efficiency, higher reliability and broad frequency bandwidth compared with traditional rack pinion backpack energy harvester. We have conducted experiment to show advantages of MMR based backpack energy harvester. We recruited four male subjects for the test, since male and female have different figure characteristics and we only designed one frame according to male figures. Subjects were asked to wear backpack frame we designed which also embedded the harvesters to walk with different speed on the treadmill. Two types of harvesters have also been tested and compared. The advantages of MMR based backpack energy harvester compared with traditional backpack energy harvester have been presented.

5.2 Human test

5.2.1 Human test setup and procedure

Four male volunteers agreed to participate in the study. However, only two male volunteers were able to finish full series of test with different resistors walking on different speed because we need several days schedule of tests or even several week since subjects need to get enough rest for tests. During the tests, the subjects were asked to carry the energy harvesting backpack and walk on a treadmill with two different speeds, including 3 and 3.5 mph. In each walking speed, the generator was shunted with four different resistor values, including 1.19, 2.31, 2.7, 5 Ω. Furthermore, the voltage and relative displacement were continuously recorded by CoCo - 80 vibration data collector during the tests. The overall plan was for the subjects to walk on the treadmill while they were carrying the backpack frame with two types of harvesters (MMR based energy harvester and traditional energy harvester) which the subjects were completely blind test. The study was approved by the departmental ethics review committee. All the data recordings were begun after around 1min or when the backpack was observing at the steady state condition. Each set of experiment will record two sets of data, and each set of data will last at least 10s.

Between two types of harvesters, the subjects could take off the backpack and have a rest for at least 10min. In addition, we also recorded video for human COM motion by a CANON camera. A small black marker around 1 cm * 1 cm will be taped on hipbone outside the clothes.

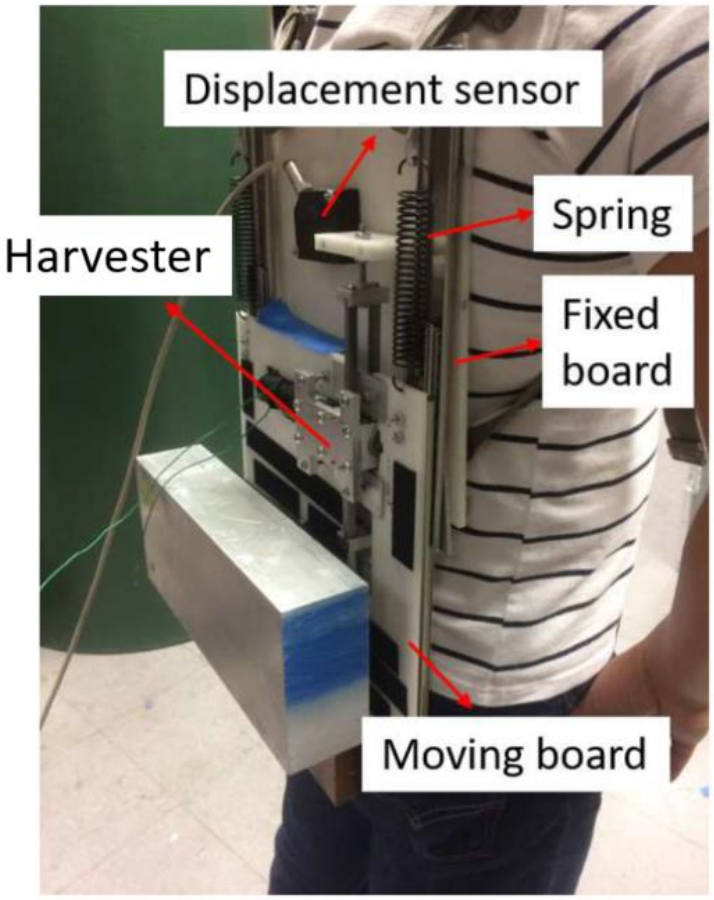

Figure 5-1. Backpack frame worn on a male. The harvester was installed in the cutout of the moving board and the racks are fixed to the fixed board.

5.2.2 Human test results and discussion

Figure 5-2 shows the average power vs. different resistors of both subjects wearing the MMR-based and traditional backpack harvester, respectively, and walking at different speeds. There are several things worth noting. First of all, it can be seen that, the MMR-based backpack harvester generate more power from both subjects regardless of resistor values and walking speeds. This demonstrates the influence of mechanical motion rectification on power efficiency. Second, power generation is proportional to walking speed. Third, each backpack harvester has a different trend of power generation with respect to resistors. For the traditional one, the power reaches its

maximum after 2.7 Ω and maintains approximately constant afterwards. On the other hand, the MMR-based one shows increasing trend as the resistor values increase. Finally, despite the similar trend with respect to resistor values, these two subjects generated power in different magnitudes. Subject A generated power in the range between 1 Watt to 5 Watts whereas subject B generated much less power in the range between 0.5 Watt to 3 Watts. This finding is very interesting since the tests were conducted on both subjects under identical conditions, including resistor values, walking speeds, and backpack types. The discrepancy may be related to different walking gaits of these two subjects. During the tests, subject A was walking with a faster pace and maintained his upper body upright for most of the time. Subject B, on the other hand, was walking with a slower pace and tend to lean forward when walking at the same speeds.

Figure 5-3 and Figure 5-4 shows the steady state data of subject A walking at 3mph and 3.5mph with a 5.24 Ω. While walking at 3mph, the average power output with MMR energy harvester over 10s is 4.02 W and with traditional energy harvester is 2.60W. While walking with 3.5mph, the average power with MMR energy harvester over 10s is 4.84W and the maximum instant power is 12.8W, however, with traditional energy harvester is only 1.55W. There are few things we could notice from the data that the upward displacement and the downward displacement is not the same, which means that the relative displacement is unsymmetrical, which might be influenced by unsymmetrical vertical COM motion. It led to one large and following by one small peak power value in one cycle.

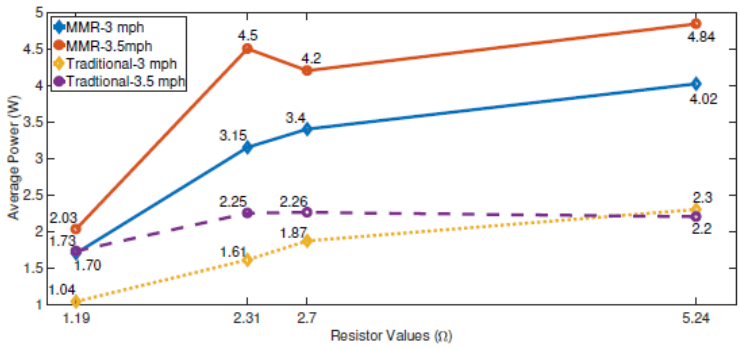

(a) Subject A

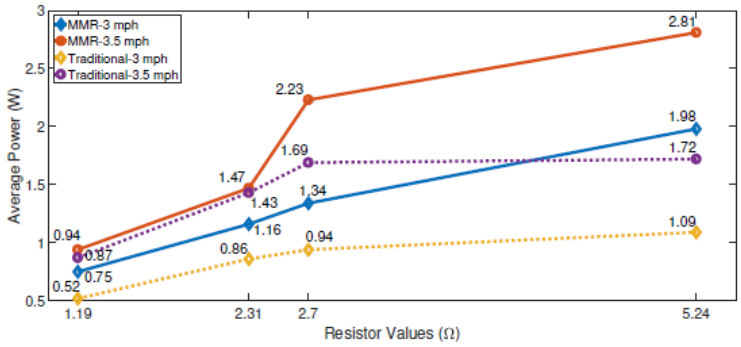

(b) Subject B

Figure 5-2. Traditional energy harvesting backpack tests: measured average power vs. different resistor values. The average power is calculated over an interval of 10 s.

(a) *(b)*

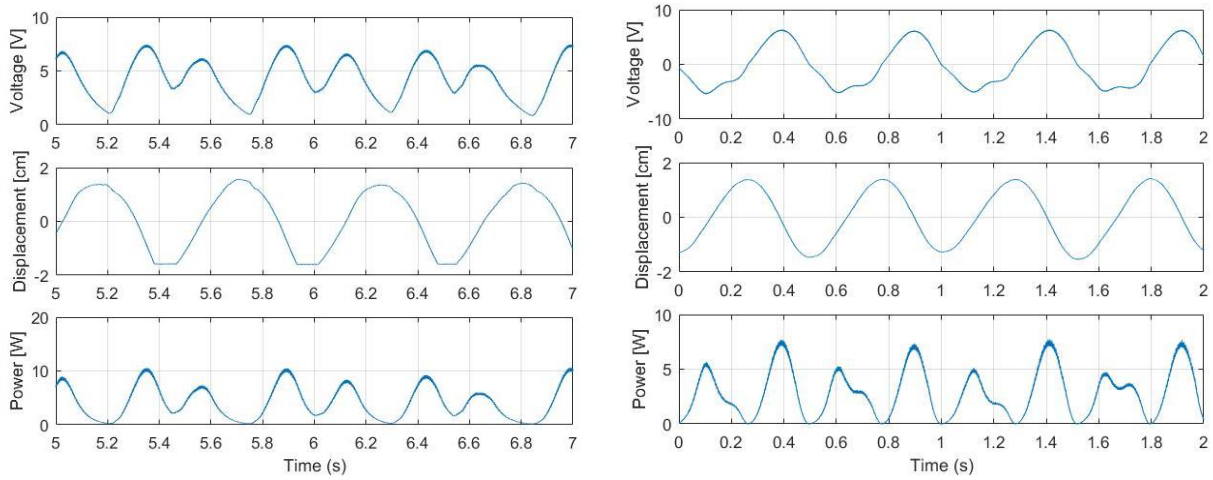

Figure 5-3. Voltage output, measured relative displacement and power by subject A walking at 3mph with 5.24Ω external resistor: (a) MMR energy harvester; (b) traditional energy harvester.

(a) *(b)*

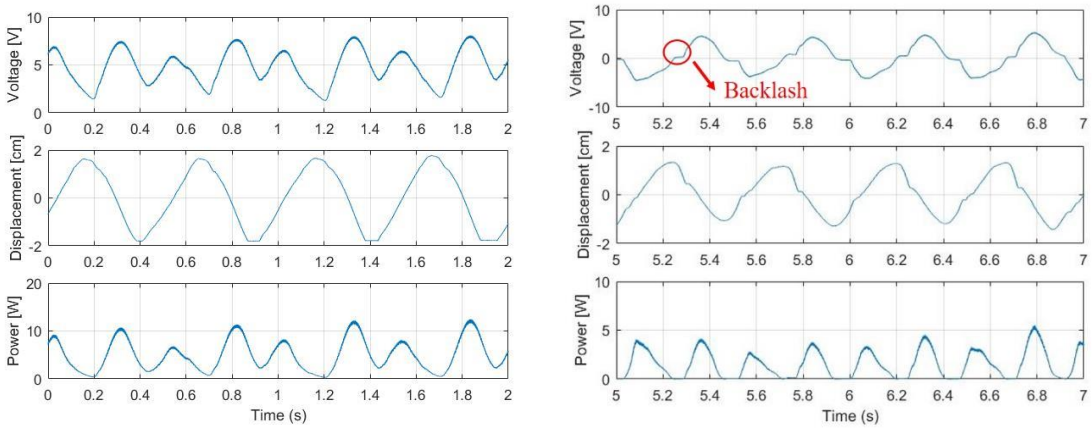

Figure 5-4. Measured relative displacement, voltage output and power by subject A walking at 3.5mph with 5.24Ω external resistor: (a) MMR energy harvester; (b) traditional energy harvester.

5.2.3 Human vertical COM results

In order to study effect of different energy harvesters to human COM motion, we have recorded videos during subjects doing experiments. The camera stands outside the treadmill and one set square was been taped on one of treadmill grips for calibration. The videos were processed into frames and the marker we have attached on the subjects body has been tracked using a software called 'Tracker'. Even though the software could calibrate images and we tried to tape the marker at the same position each time, the marker could not be at the same spot for different subjects and might not be at the exact hipbone point. Vertical COM motion we processed from videos still have might have some difference in the actual vertical COM motion.

Figure 5-5 shows vertical COM motion from subject A's results with 3mph and 3.5mph walking speed with 5.24 Ω external resistor in time domain from the processed videos. As we can see from Figure 5-5 (a) and (b) of subject A with MMR based energy harvester with 5.24Ω external resistor walking in 3mph and 3.5mph. Compare with (a) and (b), there is no significant value difference in peak to peak vertical COM motion. Figure 5-5 (c) and (d) shows the result of vertical COM motion of subject A in time domain with traditional energy harvester with 5.24Ω external resistor walking in 3mph and 3.5mph. Compared with (a) and (c), (b) and (d), there is also no significant value difference in peak to peak vertical COM motion. There is no significant evidence shown the trend of vertical COM motion changes with different walking speed, 3mph and 3.5mph, and different

types of harvester, MMR based backpack energy harvester and traditional energy harvester in our experiment result.

(a)

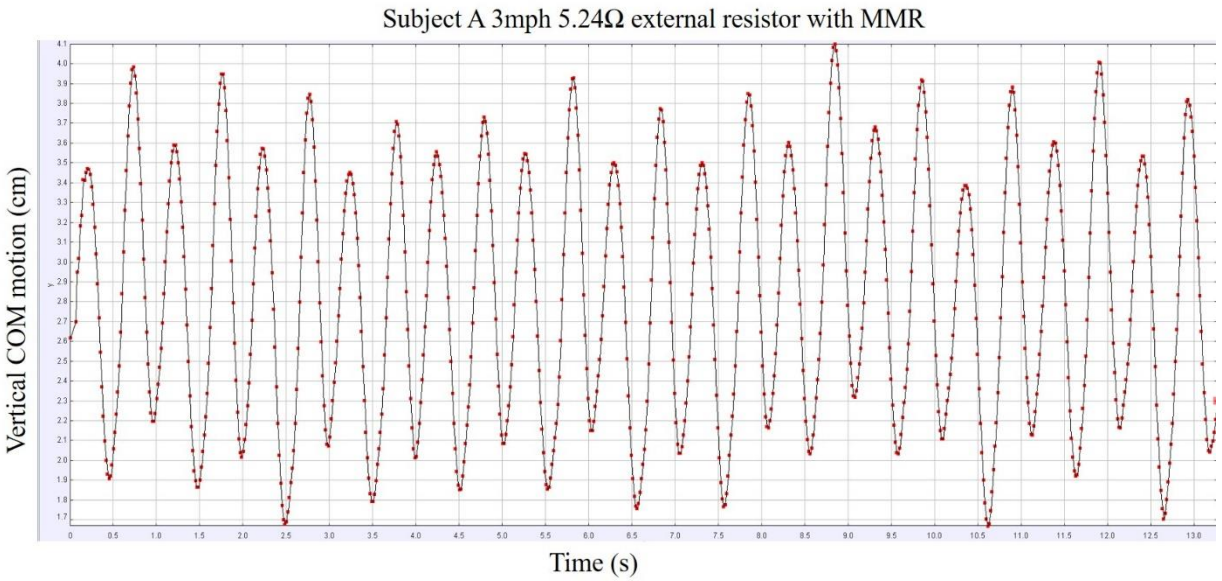

(b)

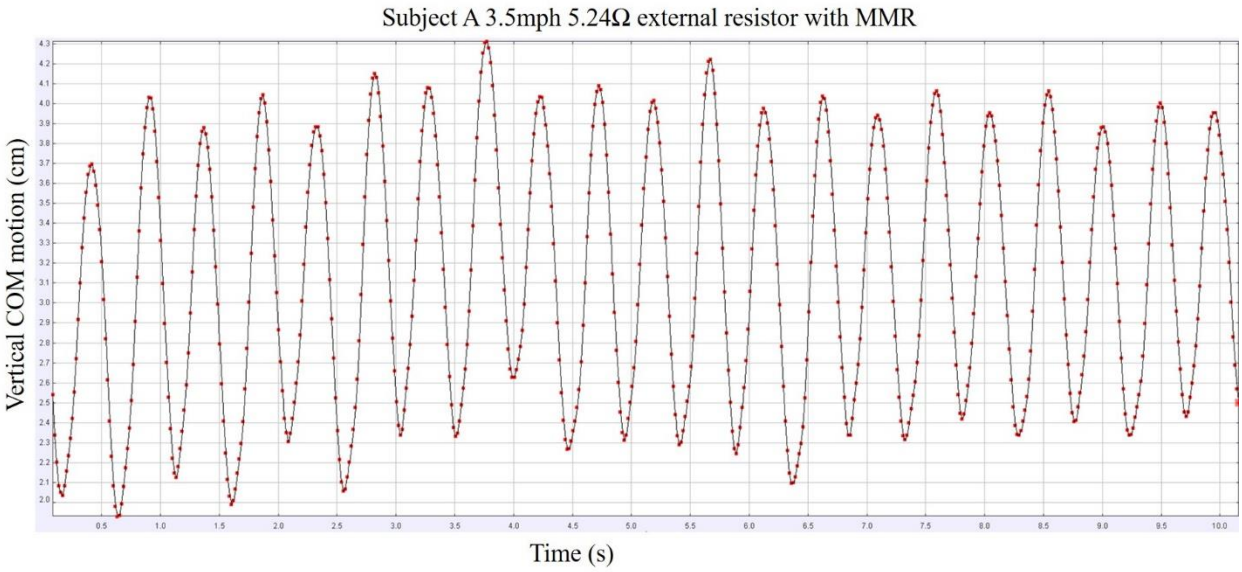

(c)

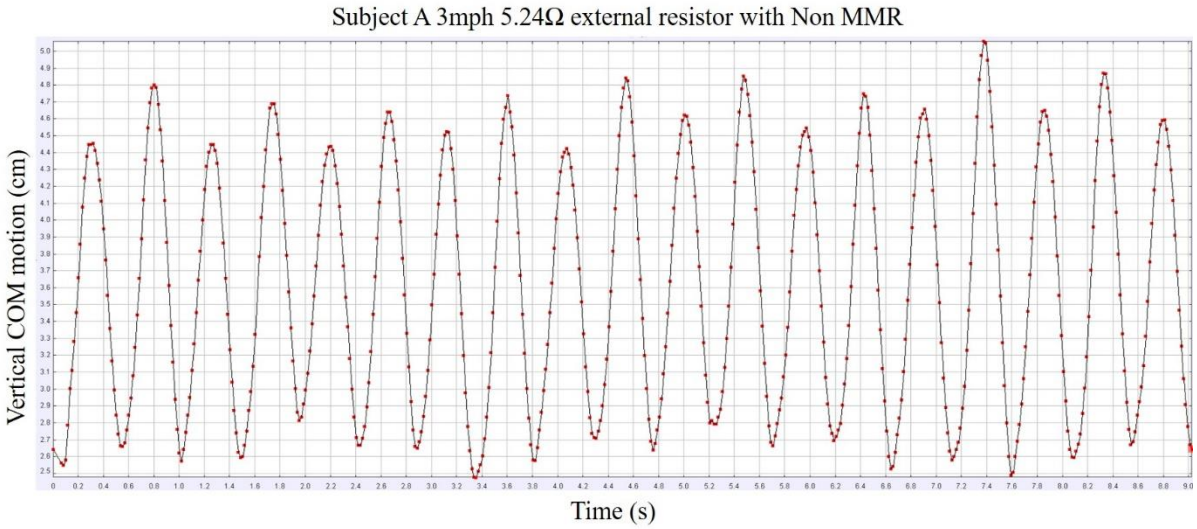

(d)

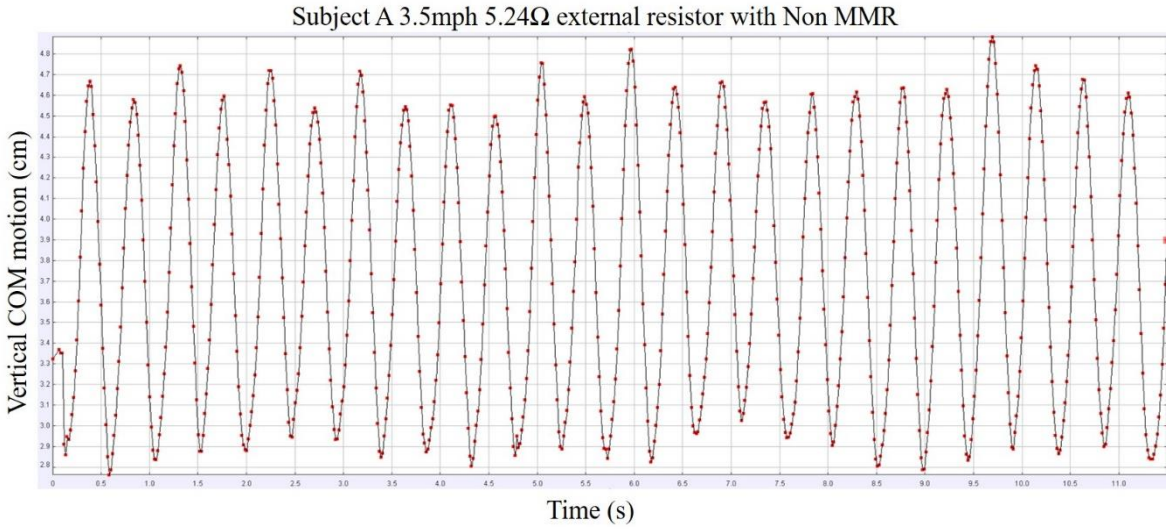

Figure 5-5. Tracked average peak to peak distance of vertical COM motion of subjects from recorded videos during experiments: (a) subject A waling with 3mph with 5.24 Ω external resistor vertical peak to peak COM motion with time wearing MMR based energy harvester; (b) subject A waling with 3.5mph with 5.24 Ω external resistor vertical peak to peak COM motion with time wearing MMR based energy harvester; (c) subject A waling with 3mph with 5.24 Ω external resistor vertical peak to peak COM motion with time wearing traditional energy harvester; (d) subject A waling with 3.5mph with 5.24 Ω external resistor vertical peak to peak COM motion with time wearing traditional energy harvester;

5.3 Chapter summary

In this chapter, experiments were conducted to compare MMR based backpack energy harvester and traditional backpack energy harvester. The human test results showed that the MMR-based backpack harvester generated more power regardless of resistor values and walking speeds. It also showed a maximum average power of 4.8 Watts and instant power of 12.8 Watts were obtained by one subject, carrying the MMR-based backpack harvester and walking at 3.5 mph. Subjects' vertical COM mass motion has also been recorded and been discussed in Chapter 5.2.3.

After comparing with two models we have introduced in last few chapters, dual mass model and bipedal model, we could concluded our results of MMR energy harvester and traditional energy harvester along with our experiment result as following table.

Table 5-1 Concluded results of dual mass model, bipedal model and experimental results.

	Dual mass model (ζ_m =10%)	Bipedal model (ζ_m =10%)	Experiment
Optimal with MMR harvester power	6.93 W	9.05 W	4.84 W
Optimal with traditional harvester power	5.63 W	6.17 W	2.81 W

6. Conclusion and future work

6.1 Conclusions of the Thesis

This thesis demonstrated the design, manufacture and modeling of new generation MMR based backpack energy harvester. We compared MMR based backpack energy harvester with traditional backpack energy harvesters.

1. With simple dual mass model, MMR based energy harvester has an absolute advantage over the other two types, pure damping energy harvester and traditional rack pinion based energy

harvester, in the power output at low electrical damping ratio ζ_e with up to 28.6W average power. We also take the human comfort factor into consideration. By comparing human peak force of these three types of harvesters, non MMR harvester has the smallest minimum value, but in certain range of tuning ratio ($0.98 < f < 2.2$), the MMR based harvester is more comfortable to human body. To better understand the tradeoff relationship between human comfort and harvester power output, we introduced a new term called 'Human harvester efficiency'. In the human harvester efficiency comparison, overall, pure viscous system costs more additional human metabolic cost than the other two systems when generate the same amount of electrical power output when $\zeta_e = 0.2$. When $f \leq 0.8$, MMR system has the smallest human harvester efficiency value. When increase mechanical damping ratio in the harvester system, the optimal power value significantly decreased and tuning ratio at the optimal power point kept the same as when mechanical damping ratio is 1%, but the electrical damping ratio at the optimal power point is different than 1% mechanical damping ratio case.

2. Since the limitations of simple dual mass system, we developed the new bipedal walking with suspended load backpack model. There are seven parameters in the bipedal model. The stability of this model has also been discussed.
3. With the new bipedal walking with suspended load model, we compared power output of MMR based backpack energy harvester with traditional rack pinion based energy harvester. MMR based backpack energy harvester has larger average power output in different conditions. We analyzed vertical COM motion results from the bipedal walking model in frequency domain and concluded that the vertical COM motion has multiple frequency content including high frequency, which might be one of the reasons result from MMR based backpack energy harvester always has larger power output.
4. Experiments were conducted to verify the advantages of MMR based backpack energy harvester, high power output, high efficiency, and high reliability. Up to 4.84W power output was achieved by MMR based backpack energy harvester while walking on treadmill with 3.5mph. Vertical COM motion of subjects during experiment have also been processed and discussed.

6.2 Recommendations for Future Research

The recommendations for future study can be concluded as follows,

1. The bipedal walking with suspended load model still has some drawbacks like overestimating vertical COM motion. There is still room we could do to improve this model:
    - **a.** Put MMR based harvester models in improved bipedal walking model.
    - **b.** Adjust other human dynamics parameter to study like human leg spring stiffness in the future study.
    - **c.** This model overestimated the human vertical COM motion.
    - **d.** The human walking gait does not have stable steady state solution when average walking speed higher than 1.2 m/s. Even with improved bipedal walking model, the walking speed in the simulation could not higher than 1.56 m/s.
2. Human's comfort needs to be considered and needs to think some factors to evaluate comfort in the bipedal model.

References:

[1]	WD McArdle, FI Katch, VL Katch, Exercise Physiology: Energy, Nutrition, and Human Performance. 5 edition, New York, NY: Lippincott, Williams & Wilkins, 2001.
[2]	D. Winter, Biomechanics and motor control of human movement. 3 edition, Hoboken, NJ: John Wiley and Sons, 2005.
[3]	S. Chen, "Dynamoelectric shoes". US Patent 5495682, 1996.
[4]	JM Donelan, Q Li, V Niang, JA Hoffer, DJ Weber, AD Kuo, "Generating Electricity During Walking with Minimal User Effort," Sicence, pp. 807-810, 2008.
[5]	L Rome, EM Goldman and TD Yoo, "Generating electricity while walking with loads," Science, vol. 309, pp. 1725-1728, 2005.
[6]	Starner, Thad. "Human-powered wearable computing." IBM systems Journal 35.3.4 (1996): 618-629.
[7]	Paradiso, Joseph A., and Thad Starner. "Energy scavenging for mobile and wireless electronics." IEEE Pervasive computing 4.1 (2005): 18-27.
[8]	Winter, David A. Biomechanics and motor control of human movement. John Wiley & Sons, 2009.
[9]	Riemer, Raziel, and Amir Shapiro. "Biomechanical energy harvesting from human motion: theory, state of the art, design guidelines, and future directions." Journal of neuroengineering and rehabilitation 8.1 (2011): 22.
[10]	Davidson, Paul R., and Daniel M. Wolpert. "Widespread access to predictive models in the motor system: a short review." Journal of Neural Engineering 2.3 (2005): S313.
[11]	Zarrugh, M. Y., F. N. Todd, and H. J. Ralston. "Optimization of energy expenditure during level walking." European Journal of Applied Physiology and Occupational Physiology 33.4 (1974): 293-306.
[12]	Collins, Steven H., Peter G. Adamczyk, and Arthur D. Kuo. "Dynamic arm swinging in human walking." Proceedings of the Royal Society of London B: Biological Sciences 276.1673 (2009): 3679-3688.
[13]	Harman, Everett, et al. The effects of backpack weight on the biomechanics of load carriage. No. USARIEM-T00-17. ARMY RESEARCH INST OF ENVIRONMENTAL MEDICINE NATICK MA MILITARY PERFORMANCEDIV, 2000.
[14]	Hicks-Little, Charlie A. A lower extremity kinematic analysis of stair ascent and descent in osteoarthritic knees. ProQuest, 2008.
[15]	The Knee During Gait http://www.utdallas.edu/atec/midori/Handouts/walkingGraphs.htm

[16]	Shenck, Nathan S., and Joseph A. Paradiso. "Energy scavenging with shoe-mounted piezoelectrics." IEEE micro 21.3 (2001): 30-42.
[17]	Xie, Longhan, and Mingjing Cai. "An in-shoe harvester with motion magnification for scavenging energy from human foot strike." IEEE/ASME Transactions on Mechatronics 20.6 (2015): 3264-3268.
[18]	Guo, Lukai, and Qing Lu. "Potentials of piezoelectric and thermoelectric technologies for harvesting energy from pavements." Renewable and Sustainable Energy Reviews 72 (2017): 761-773.
[19]	Kuang, Yang, et al. "Energy harvesting during human walking to power a wireless sensor node." Sensors and Actuators A: Physical 254 (2017): 69-77.
[20]	Kuo, Arthur D. "Harvesting energy by improving the economy of human walking." Science 309.5741 (2005): 1686-1687.
[21]	Grabowski, Alena, Claire T. Farley, and Rodger Kram. "Independent metabolic costs of supporting body weight and accelerating body mass during walking." Journal of Applied Physiology 98.2 (2005): 579-583.
[22]	Donelan, J. Maxwell, Rodger Kram, and Arthur D. Kuo. "Mechanical work for step-to-step transitions is a major determinant of the metabolic cost of human walking." Journal of Experimental Biology 205.23 (2002): 3717-3727.
[23]	Rome, Lawrence C., Louis Flynn, and Taeseung D. Yoo. "Biomechanics: Rubber bands reduce the cost of carrying loads." Nature 444.7122 (2006): 1023-1024.
[24]	Kram, R. O. D. G. E. R. "Carrying loads with springy poles." Journal of Applied Physiology 71.3 (1991): 1119-1122.
[25]	Li, Zhongjie, et al. "Energy-harvesting shock absorber with a mechanical motion rectifier." Smart Materials and Structures 22.2 (2012): 025008.
[26]	Lin, Teng, Lirong Wang, and Lei Zuo. "Anchorless Design of Electromagnetic Vibration Energy Harvester for Railroad." ASME 2015 Dynamic Systems and Control Conference. American Society of Mechanical Engineers, 2015.
[27]	Liang, Changwei, You Wu, and Lei Zuo. "Vibration energy harvesting system with mechanical motion rectifier." ASME 2015 Dynamic Systems and Control Conference. American Society of Mechanical Engineers, 2015.
[28]	Liang, Changwei, You Wu, and Lei Zuo. "Broadband pendulum energy harvester." Smart Materials and Structures 25.9 (2016): 095042.

[29]	Knapik, Joseph J., Katy L. Reynolds, and Everett Harman. "Soldier load carriage: historical, physiological, biomechanical, and medical aspects." Military medicine 169.1 (2004): 45.
[30]	http://www.cerdec.army.mil/news_and_media/Energy_Harvesting_Assault_Pack/
[31]	T. Casey, "Wrap Your Brain Around A Backpack That Creates Electricity," Clean Technica, 03 11 2014. [Online]. Available: http://cleantechnica.com/2014/11/03/wrap-your-brain-around-this-electric-backpack/. [Accessed 14 12 2015].
[32]	Liang, Changwei, Junxiao Ai, and Lei Zuo. "Design, Fabrication, Simulation and Testing of a Novel Ocean Wave Energy Converter." ASME 2015 International Manufacturing Science and Engineering Conference. American Society of Mechanical Engineers, 2015.
[33]	Inman, Verne Thompson, Henry James Ralston, and Frank Todd. Human walking. Williams & Wilkins, 1981.
[34]	Zhang, L., et al. "Stiffness and viscous damping of the human leg." Proc. of the 24th Ann. Meeting of the Am. Soc. of Biomech., Chicago, IL. 2000.
[35]	Tang, Xiudong, and Lei Zuo. "Enhanced Design of Vibration Energy Harvester Using Dual Masses." ASME 2011 International Design Engineering Technical Conferences and Computers and Information in Engineering Conference. American Society of Mechanical Engineers, 2011.
[36]	Guo, Sijing, et al. "Performances of Energy-Harvesting Shock Absorbers on Various Types of Vehicles." ASME 2015 Dynamic Systems and Control Conference. American Society of Mechanical Engineers, 2015.
[37]	Yuan, Yue, and Lei Zuo. "Dynamics of energy harvesting backpack with human being interaction." SPIE Smart Structures and Materials+ Nondestructive Evaluation and Health Monitoring. International Society for Optics and Photonics, 2016.
[38]	Ackerman, Jeffrey, and Justin Seipel. "Energetics of bio-inspired legged robot locomotion with elastically-suspended loads." 2011 IEEE/RSJ International Conference on Intelligent Robots and Systems. IEEE, 2011.
[39]	Compliant leg behaviour explains basic dynamics of walking and running." Proceedings of the Royal Society of London B: Biological Sciences 273.1603 (2006): 2861-2867.
[40]	Kuo, Arthur D., J. Maxwell Donelan, and Andy Ruina. "Energetic consequences of walking like an inverted pendulum: step-to-step transitions." Exercise and sport sciences reviews 33.2 (2005): 88-97.
[41]	Kuo, Arthur D., J. Maxwell Donelan, and Andy Ruina. "Energetic consequences of walking like an inverted pendulum: step-to-step transitions." Exercise and sport sciences reviews 33.2 (2005): 88-97.

[42]	Rummel, Juergen, et al. "Stable and robust walking with compliant legs." ICRA. 2010.